Green Fluorescent Protein as a Marker for Gene Expression
Author(s): Martin Chalfie, Yuan Tu, Ghia Euskirchen, William W. Ward and Douglas C. Prasher
Source: *Science*, New Series, Vol. 263, No. 5148 (Feb. 11, 1994), pp. 802-805
Published by: American Association for the Advancement of Science
Stable URL: http://www.jstor.org/stable/2882924
Accessed: 19-09-2016 19:39 UTC

sample is extracted from the ampoule and cleaned of the surrounding excess impregnant by standard mechanical polishing techniques. In this way, we prepared nanowires of various metals (In, Sn, and Al) and semiconductors (Se, Te, GaSb, and Bi_2Te_3) (Fig. 2).

The nanowire composites create substantial electric field patterns over the sample surface. We used a scanning probe microscope to measure electric fields at the surface of a nanocomposite. In a NanoScope (Digital Instruments, Santa Barbara, California) scanning force microscope, the sample is mounted with conductive epoxy to a metal holder and is held at a few volts relative to a conductive cantilever tip that is grounded. The metal-coated, etched, single-crystal silicon tip has a radius of curvature of about 5 nm. The tip is set to oscillate at a frequency near its resonance frequency (78 kHz). When the cantilever encounters a vertical electric field gradient, the effective spring constant is modified, shifting its resonance frequency. By recording the amplitude of the cantilever oscillations while scanning the sample surface, we obtain an image that reveals the strength of the electric force gradient (*13, 14*).

The image, however, may also contain topographical information; it is difficult to separate the two effects. This is circumvented by taking measurements in two passes over each scan line (*15*). On the first pass, a topographical image (Fig. 3A) is taken with the cantilever tapping the surface, and the information is stored in memory. On the second pass, the tip is lifted to a selected separation between the tip and local surface topography (typically 20 to 200 nm), such that the tip does not touch the surface. By using the stored topographical data instead of the standard feedback, we can keep the separation constant. In this second pass, cantilever oscillation amplitudes are sensitive to electric force gradients without being influenced by topographic features (Fig. 3B). This two-pass measurement process is recorded for every scan line, producing separate topographic and electric force images. From these images, contours of electric force gradient (Fig. 3C) can be drawn.

The amplitude of the cantilever oscillations is very large for small lift heights, and the images fade at separations larger than 80 nm. This is consistent with previous reports of a strong dependence of the tip-surface force on the vertical separation (*13*). More work needs to be done to understand this quantitatively. Note that some of the nanowires that appear in the topographic image are missing from the electric field image (Fig. 3). This is because either electrical contact to these nanowires has failed or electrical conduction along the wire length has been interrupted. The scanning force technique thus provides a unique way of mapping the electrical properties of nanocomposites.

Applications of the metal nanowire composites include high-density electrical multifeedthroughs and high-resolution plates for transferring a two-dimensional charge distribution between microelectronic devices. The semiconductor nanowires can be used in photodetector arrays of high spatial resolution, where each wire acts as a pixel of submicrometer dimensions. Also, with the application of the injection technique to ultrasmall channel insulators (channel diameter less than 50 nm) (*16, 17*), nanowire arrays can be made for fundamental studies of a variety of phenomena, such as quantum confinement of charge carriers and mesoscopic transport.

REFERENCES AND NOTES

1. An overview can be found in M. J. Yacaman, T. Tsakalakos, B. H. Kear, Eds., *Nanostruct. Mat.* **3** (nos. 1–6) (1993).
2. R. Roy, *Nanophase and Nanocomposite Materials*, S. Komarneni, J. C. Parker, G. J. Thomas, Eds. (Mat. Res. Soc. Symp. Proc. 286, Materials Research Society, Pittsburgh, PA, 1993), pp. 241–250, and references therein.
3. Early work on the preparation of ultrathin superconducting wires by injection of nanochannel matrices was done by W. G. Schmidt and R. J. Charles [*J. Appl. Phys.* **35**, 2552 (1964)] and by V. N. Bogomolov [*Sov. Phys. Usp.* **21**, 77 (1978)].
4. C. A. Huber and T. E. Huber, *J. Appl. Phys.* **64**, 6588 (1988).
5. N. F. Borrelli and J. C. Luong, *Proc. SPIE* **866**, 104 (1988).
6. B. L. Justus, R. J. Tonucci, A. D. Berry, *Appl. Phys. Lett.* **61**, 3151 (1992).
7. M. J. Tierney and C. R. Martin, *J. Phys. Chem.* **93**, 2878 (1989).
8. G. D. Stucky and J. E. Mac Dougall, *Science* **247**, 669 (1990), and references therein.
9. P. M. Ajayan and S. Iijima, *Nature* **361**, 333 (1993).
10. An array of parallel metal cylinders would be transparent to light that had a wavelength much larger than the cylinder diameter and separation and propagated along the cylinder axis [D. E. Aspnes, A. Heller, J. D. Porter, *J. Appl. Phys.* **60**, 3028 (1986)].
11. Whatman Laboratory Division, Clifton, NJ.
12. J. W. Diggle, T. C. Downie, C. W. Goulding, *J. Electrochem. Soc.* **69**, 365 (1969).
13. Y. Martin, D. W. Abraham, H. K. Wickramasinghe, *Appl. Phys. Lett.* **52**, 1103 (1988).
14. J. E. Stern, B. D. Terris, H. J. Maimin, D. Rugar, *ibid.* **53**, 2717 (1988).
15. Lift Mode operation, Digital Instruments, Inc., Santa Barbara, CA (patent pending).
16. R. C. Furneaux, W. R. Rigby, A. P. Davidson, *Nature* **337**, 147 (1989).
17. R. J. Tonucci, B. L. Justus, A. J. Campillo, C. E. Ford, *Science* **258**, 783 (1992).

18. We thank V. Elings for valuable discussions, B. Schardt and S. Thedford for image processing, and S. Nourbakhsh for electron microscopy. This work was supported by the Army Research Office, the Independent Research Program of the Office of Naval Research, and the National Science Foundation.

22 October 1993; accepted 20 December 1993

Green Fluorescent Protein as a Marker for Gene Expression

Martin Chalfie,* Yuan Tu, Ghia Euskirchen, William W. Ward, Douglas C. Prasher†

A complementary DNA for the *Aequorea victoria* green fluorescent protein (GFP) produces a fluorescent product when expressed in prokaryotic (*Escherichia coli*) or eukaryotic (*Caenorhabditis elegans*) cells. Because exogenous substrates and cofactors are not required for this fluorescence, GFP expression can be used to monitor gene expression and protein localization in living organisms.

Light is produced by the bioluminescent jellyfish *Aequorea victoria* when calcium binds to the photoprotein aequorin (*1*). Although activation of aequorin in vitro or in heterologous cells produces blue light, the jellyfish produces green light. This light is the result of a second protein in *A. victoria* that derives its excitation energy from aequorin (*2*), the green fluorescent protein (GFP).

Purified GFP, a protein of 238 amino acids (*3*), absorbs blue light (maximally at 395 nm with a minor peak at 470 nm) and emits green light (peak emission at 509 nm with a shoulder at 540 nm) (*2, 4*). This fluorescence is very stable, and virtually no photobleaching is observed (*5*). Although the intact protein is needed for fluorescence, the same absorption spectral properties found in the denatured protein are found in a hexapeptide that starts at amino acid 64 (*6, 7*). The GFP chromophore is derived from the primary amino acid sequence through the cyclization of serine-dehydrotyrosine-glycine within this hexapeptide (*7*). The mechanisms that produce the dehydrotyrosine and cyclize the poly-

M. Chalfie, Y. Tu, G. Euskirchen, Department of Biological Sciences, Columbia University, New York, NY 10027, USA.
W. W. Ward, Department of Biochemistry and Microbiology, Cook College, Rutgers University, New Brunswick, NJ 08903, USA.
D. C. Prasher, Biology Department, Woods Hole Oceanographic Institution, Woods Hole, MA 02543, USA.

*To whom correspondence should be addressed.
†Present address: U.S. Department of Agriculture, Building 1398, Otis Air National Guard Base, MA 02542, USA.

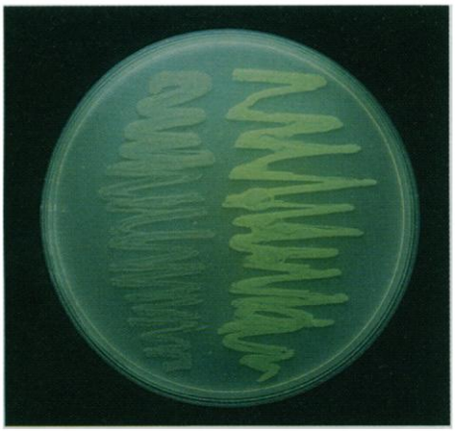

Fig. 1. Expression of GFP in *E. coli*. The bacteria on the right side of the figure have the GFP expression plasmid. Cells were photographed during irradiation with a hand-held long-wave UV source.

peptide to form the chromophore are unknown. To determine whether additional factors from *A. victoria* were needed for the production of the fluorescent protein, we tested GFP fluorescence in heterologous systems. Here, we show that GFP expressed in prokaryotic and eukaryotic cells is capable of producing a strong green fluorescence when excited by blue light. Because this fluorescence requires no additional gene products from *A. victoria*, chromophore formation is not species-specific and occurs either through the use of ubiquitous cellular components or by autocatalysis.

Expression of GFP in *Escherichia coli* (8) under the control of the T7 promoter results in a readily detected green fluorescence (9) that is not observed in control bacteria. Upon illumination with a long-wave ultraviolet (UV) source, fluorescent bacteria were detected on plates that contained the inducer isopropyl-β-D-thiogalactoside (IPTG) (Fig. 1). Because the cells grew well in the continual presence of the inducer, GFP did not appear to have a toxic effect on the cells. When GFP was partially purified from this strain (*10*), it was found to have fluorescence excitation and emission spectra indistinguishable from those of the purified native protein (Fig. 2). The spectral properties of the recombinant GFP suggest that the chromophore can form in the absence of other *A. victoria* products.

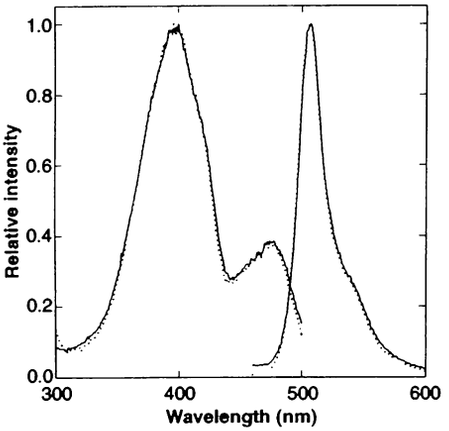

Fig. 2. Excitation and emission spectra of *E. coli*–generated GFP (solid lines) and purified *A. victoria* L form GFP (dotted lines).

Transformation of the nematode *Caenorhabditis elegans* also resulted in the production of fluorescent GFP (*11*) (Fig. 3). GFP was expressed in a small number of neurons under the control of a promoter for the *mec-7* gene. The *mec-7* gene encodes a β-tubulin (*12*) that is abundant in six touch receptor neurons in *C. elegans* and less abundant in a few other neurons (*13, 14*). The pattern of expression of GFP was similar to that detected by MEC-7 antibody or from *mec-7–lacZ* fusions (*13–15*). The strongest fluorescence was seen in the cell bodies of the four embryonically derived touch receptor neurons (ALML, ALMR, PLML, and PLMR) in younger larvae. The processes from these cells, including their terminal branches, were often visible in larval animals. In some newly hatched animals, the PLM processes were short and ended in what appeared to be prominent growth cones. In older larvae, the cell bodies of the remaining touch cells (AVM and PVM) were also seen; the processes of these cells were more difficult to detect. These postembryonically derived cells arise during the first of the four larval stages (*16*), but their outgrowth occurs in the following larval stages (*17*), with the cells becoming functional during the fourth larval stage (*18*). The fluorescence of GFP in these cells is consistent with these previous results: no fluorescence was detected in these cells in newly hatched or late first-stage larvae, but fluorescence was seen in four of ten late second-stage larvae, all nine early fourth-stage larvae, and seven of eight young adults (*19*). In addition, moderate to weak fluorescence was seen in a few other neurons (Fig. 3) (*20*).

Like the native protein, GFP expressed in both *E. coli* and *C. elegans* is quite stable (lasting at least 10 min) when illuminated with 450- to 490-nm light. Some photobleaching occurs, however, when the cells are illuminated with 340- to 390-nm or 395- to 440-nm light (*21*).

Several methods are available to monitor gene activity and protein distribution within cells. These include the formation of fusion proteins with coding sequences for β-galactosidase, firefly luciferase, and bacterial luciferase (*22*). Because such methods require exogenously added substrates or cofactors, they are of limited use with living tissue. Because the detection of intracellular GFP requires only irradiation by near UV or blue light, it is not limited by the availability of substrates. Thus, it should provide an excellent means for monitoring gene expression and protein localization in living cells (*23, 24*). Because it does not appear to interfere with cell growth and function, GFP should also be a convenient indicator of transformation and one that could allow cells to be separated with fluorescence-activated cell sorting. We also envision that GFP can be used as a vital marker so that cell growth (for example, the elaboration of neuronal processes) and movement can be followed in situ, especially in animals that are essentially transparent like *C. elegans* and zebra fish. The relatively small size of the protein may facilitate its diffusion throughout the cytoplasm of extensively branched cells like neurons and glia. Because the GFP fluorescence persists after treatment with formaldehyde (9), fixed preparations can also be examined. In addition, absorption of appropriate laser light by GFP-expressing cells (as has been done for Lucifer Yellow–containing cells) (*25*) could result in the selective killing of the cells.

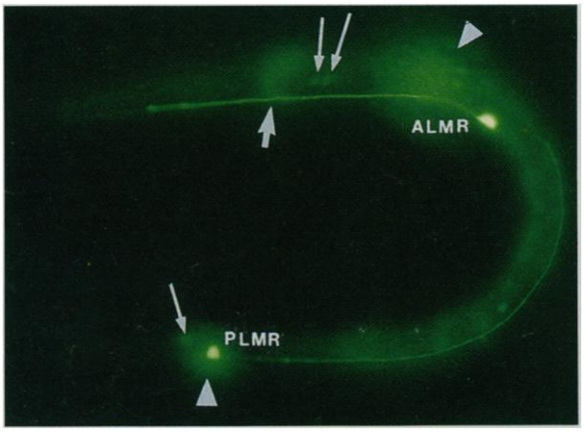

Fig. 3. Expression of GFP in a first-stage *C. elegans* larva. Two touch receptor neurons (ALMR and PLMR) are labeled at their strongly fluorescing cell bodies. Processes can be seen projecting from both of these cell bodies. Halos produced from the out-of-focus homologs of these cells on the other side of the animal are indicated by arrowheads. The thick arrow points to the nerve ring branch from the ALMR cell (out of focus); thin arrows point to weakly fluorescing cell bodies. The background fluorescence is the result of the animal's autofluorescence.

REFERENCES AND NOTES

1. O. Shimomura, F. H. Johnson, Y. Saiga, *J. Cell. Comp. Physiol.* **59**, 223 (1962).
2. J. G. Morin and J. W. Hastings, *J. Cell. Physiol.* **77**, 313 (1971); H. Morise, O. Shimomura, F. H. Johnson, J. Winant, *Biochemistry* **13**, 2656 (1974).
3. D. C. Prasher, V. K. Eckenrode, W. W. Ward, F. G. Prendergast, M. J. Cormier, *Gene* **111**, 229 (1992).
4. W. W. Ward, C. W. Cody, R. C. Hart, M. J. Cormier, *Photochem. Photobiol.* **31**, 611 (1980).
5. F. G. Prendergast, personal communication.
6. O. Shimomura, *FEBS Lett.* **104**, 220 (1979).
7. C. W. Cody, D. C. Prasher, W. M. Westler, F. G. Prendergast, W. W. Ward, *Biochemistry* **32**, 1212 (1993).
8. Plasmid pGFP10.1 contains the Eco RI fragment encoding the GFP complementary DNA (cDNA) from λ*gfp*10 (*3*) in pBS(+) (Stratagene). The fragment was obtained by amplification with the polymerase chain reaction (PCR) [R. K. Saiki *et al.*, *Science* **239**, 487 (1988)] with primers flanking the Eco RI sites and subsequent digestion with Eco RI. DNA was prepared by the Magic Minipreps procedure (Promega) and sequenced (after an additional ethanol precipitation) on an Applied Biosystems DNA Sequencer 370A at the DNA sequencing facility at Columbia College of Physicians and Surgeons. The sequence of the cDNA in pGFP10.1 differs from the published sequence by a change in codon 80 within the coding sequence from CAG to CGG, a change that replaces a glutamine residue with arginine. [R. Heim, S. Emr, and R. Tsien (personal communication) first alerted us to a possible sequence change in this clone and independently noted the same change.] This replacement has no detectable effect on the spectral properties of the protein (Fig. 2). An *E. coli* expression construct was made with PCR to generate a fragment with an Nhe I site at the start of translation and an Eco RI site 5′ to the termination signal of the GFP coding sequence from pGFP10.1. The 5′ primer was ACAAAGGCTAGCAAAGGAGAAGAAC and the 3′ primer was the T3 primer (Stratagene). The Nhe I–Eco RI fragment was ligated into the similarly cut vector pET3a [A. H. Rosenberg *et al.*, *Gene* **56**, 125 (1987)] by standard methods (*26*). The resulting coding sequence substitutes an Ala for the initial GFP Met, which becomes the second amino acid in the polypeptide. The *E. coli* strain BL21 (DE3) Lys S [F. W. Studier and B. A. Moffat, *J. Mol. Biol.* **189**, 113 (1986)] was transformed with the resulting plasmid (TU#58) and grown at 37°C. Control bacteria were transformed with pET3a. Bacteria were grown on nutrient plates containing ampicillin (100 μg/ml) and 0.8 mM IPTG. [A similar PCR-generated fragment (*11*) was used in our *C. elegans* construct. As others are beginning to use pGFP10.1, we have heard that although similar PCR fragments produce a fluorescent product in other organisms (R. Heim, S. Emr, R. Tsien, personal communication; S. Wang and T. Hazelrigg, personal communication; L. Lanini and F. McKeon, personal communication) (*23*), the Eco RI fragment does not (R. Heim, S. Emr, R. Tsien, personal communication; A. Coxon, J. R. Chaillet, T. Bestor, personal communication). These results may indicate that elements at the 5′ end of the sequence or at the start of translation inhibit expression.]
9. We used a variety of microscopes (Zeiss Axiophot, Nikon Microphot FXA, and Olympus BH2-RFC and BX50) that were equipped for epifluorescence microscopy. Usually, filter sets for fluorescein isothiocyanate fluorescence were used (for example, the Zeiss filter set used a BP450-490 excitation filter, 510-nm dichroic, and either a BP515-565 or an LP520 emission filter), although for some experiments filter sets that excited at lower wavelengths were used (for example, the Zeiss filter set with BP395-440 and LP470 filters and a 460-nm dichroic or with BP340-390 and LP400 filters with a 395-nm dichroic). In some instances, a xenon lamp appeared to give a more intense fluorescence than a mercury lamp when cells were illuminated with light around 470 nm, although usually the results were comparable. No other attempts were made to enhance the signal (for example, with low-intensity light cameras), although such enhancement may be useful in some instances. Previous experiments had shown that the native protein was fluorescent after glutaraldehyde fixation (W. W. Ward, unpublished data). S. Wang and T. Hazelrigg (personal communication) (*23*) have found that GFP fusion proteins in *Drosophila melanogaster* are fluorescent after formaldehyde fixation. We have confirmed that fluorescence persists after formaldehyde fixation with our *C. elegans* animals and with recombinant GFP isolated from *E. coli*. However, the chemicals in nail polish, which is often used to seal cover slips, did appear to interfere with the *C. elegans* GFP fluorescence.
10. GFP was purified from 250-ml cultures of BL21 (DE3) Lys S bacteria containing TU#58; bacteria were grown in LB broth (*26*) containing ampicillin (100 μg/ml) and 0.8 mM IPTG. Induction was best when IPTG was present continually. Cells were washed in 4 ml of 10 mM tris-HCl (pH 7.4), 100 mM NaCl, 1 mM $MgCl_2$, and 10 mM dithiothreitol [A. Kumagai and W. G. Dunphy, *Cell* **64**, 903 (1991)] and then sonicated (two times for 20 s each) in 4 ml of the same buffer containing 0.1 mM phenylmethylsulfonyl fluoride, pepstatin A (1 μg/ml), leupeptin (1 μg/ml), and aprotinin (2 μg/ml) and centrifuged at 5000 rpm for 5 min in the cold. The supernatant was centrifuged a second time (15,000 rpm for 15 min) and then diluted sevenfold with 10 mM tris (pH 8.0), 10 mM EDTA, and 0.02% NaN_3. Corrected excitation and emission spectra were obtained with a SPEX F1T11 spectrofluorometer (Metuchen, NJ) and compared with the purified L isoprotein form of GFP from *A. victoria* (M. Cutler, A. Roth, W. W. Ward, unpublished data). The excitation spectra were measured from 300 to 500 nm with a fixed emission wavelength of 509 nm, and the emission spectra were measured from 410 to 600 nm with a fixed excitation of 395 nm. All spectra were recorded as signal-reference data (where the reference is a direct measurement of the lamp intensity with a separate photomultiplier tube) at room temperature with 1-s integration times and 1-nm increments. The spectral band widths were adjusted to 0.94 nm for all spectra.
11. Wild-type and mutant animals were grown and genetic strains were constructed according to S. Brenner [*Genetics* **77**, 71 (1974)]. The plasmid pGFP10.1 was used as a template for PCR (with the 5′ primer GAATAAAAGCTAGCAAAGATGAGTAAAG and the 3′ T3 primer) to generate a fragment with a 5′ Nhe I site (at the start of translation) and a 3′ Eco RI site (3′ of the termination codon). The DNA was cut to produce an Nhe I–Eco RI fragment that was ligated into plasmid pPD 16.51 (*12, 27*), a vector containing the promoter of the *C. elegans mec-7* gene. Wild-type *C. elegans* were transformed by coinjecting this DNA (TU#64) and the DNA for plasmid pRF4, which contains the dominant *rol-6* (*sul006*) mutation, into adult gonads as described [C. M. Mello, J. M. Kramer, D. Stinchcomb, V. Ambros, *EMBO J.* **10**, 3959 (1991)]. A relatively stable line was isolated (TU1710), and the DNA it carried was integrated as described by Mitani *et al.* (*15*) to produce the integrated elements *uIs3* and *uIs4* (in strains TU1754 and TU1755, respectively). Living animals were mounted on agar (or agarose) pads as described (*16*), often with 10 mM NaN_3 as an anesthetic (*28*) (another nematode anesthetic, phenoxypropanol, quenched the fluorescence) and examined with either a Zeiss universal or axiophot microscope. For *C. elegans*, a long-pass emission filter works best because the animal's intestinal autofluorescence (which increases as the animal matures) appears yellow (with band-pass filters the autofluorescence appears green and obscures the GFP fluorescence). Because much more intense fluorescence was seen in *uIs4* than in *uIs3* animals (for example, it was often difficult to see the processes of the ALM and PLM cells in *uIs3* animals when the animals were illuminated with a mercury lamp), the former were used for the observations reported here. The general pattern of cell body fluorescence was the same in both strains and in the parental, nonintegrated strain (fluorescence in this strain was as strong as that in the *uIs4* animals). The *uIs4* animals, however, did show an unusual phenotype: both the ALM and PLM touch cells were often displaced anteriorly. The mature cells usually had processes in the correct positions, although occasional cells had abnormally projecting processes. These cells could be identified as touch receptor cells because the fluorescence was dependent on *mec-3*, a homeobox gene that specifies touch cell fate (*13, 15, 18, 28*). Expression of *mec-7* is reduced in the ALM touch cells of the head (but not as dramatically in the PLM touch cells of the tail) in *mec-3* gene mutants (*13, 15*). We find a similar change of GFP expression in a *mec-3* mutant background for both *uIs3* and *uIs4*. Thus, GFP accurately represents the expression pattern of the *mec-7* gene. It is likely that the reduced staining in *uIs3* animals and the misplaced cells in *uIs4* animals are results of either secondary mutations or the amount or position of the integrated DNA.
12. C. Savage *et al.*, *Genes Dev.* **3**, 870 (1989).
13. M. Hamelin, I. M. Scott, J. C. Way, J. G. Culotti, *EMBO J.* **11**, 2885 (1992).
14. A. Duggan and M. Chalfie, unpublished data.
15. S. Mitani, H. P. Du, D. H. Hall, M. Driscoll, M. Chalfie, *Development* **119**, 773 (1993).
16. J. E. Sulston and H. R. Horvitz, *Dev. Biol.* **56**, 110 (1977).
17. W. W. Walthall and M. Chalfie, *Science* **239**, 643 (1988).
18. M. Chalfie and J. Sulston, *Dev. Biol.* **82**, 358 (1981).
19. In adults, the thicker size of the animals and the more intense autofluorescence of the intestine tend to obscure these cells.
20. These include several cells in the head (including the FLP cells) and tail of newly hatched animals and the BDU cells, a pair of neurons just posterior to the pharynx. Expression of *mec-7* in these cells has been seen previously (*13, 15*). The strongest staining of these non–touch receptor neurons are a pair of cells in the tail that have anteriorly directed processes that project along the dorsal muscle line. It is likely that these are the ALN cells, the sister cells to the PLM touch cells [J. G. White, E. Southgate, J. N. Thomson, S. Brenner, *Philos. Trans. R. Soc. London Ser. B* **314**, 1 (1986)].
21. The photobleaching with 395- to 440-nm light is further accelerated, to within a second, in the presence of 10 mM NaN_3, which is used as a *C. elegans* anesthetic (*11*). However, when cells in *C. elegans* have been photobleached, some recovery is seen within 10 min. Further investigation is needed to determine whether this recovery represents de novo synthesis of GFP. Rapid photobleaching (complete within a minute) of the green product was also seen when *C. elegans* was illuminated with 340- to 390-nm light. Unlike the photobleaching with 395- to 440-nm light, which abolished fluorescence produced by the 340- to 390- or 450- to 490-nm light, photobleaching with 340- to 390-nm light did not appear to affect the fluorescence produced by 395- to 490- or 450- to 490-nm light. Indeed, the fluorescence produced by 450- to 490-nm light appeared to be more intense after brief photobleaching by 340- to 390-nm light. This selective photobleaching may indicate the production of more than one fluorescent product in the animal. These data on GFP fluorescence within *E. coli* and *C. elegans* are in contrast to preliminary studies that suggest that the isolated native and *E. coli* proteins are very photostable. We do not know whether this in vivo sensitivity to photobleaching is a normal feature of the jellyfish protein (the fluorescence in *A. victoria* has not been examined) or results from the absence of a necessary posttranslational modification unique to *A. victoria*

or from nonspecific damage within the cells.
22. Reviewed in T. J. Silhavy and J. R. Beckwith, *Microbiol. Rev.* **49**, 398 (1985); S. J. Gould and S. Subramani, *Anal. Biochem.* **175**, 5 (1988); and G. S. A. B. Stewart and P. Williams, *J. Gen. Microbiol.* **138**, 1289 (1992).
23. R. Heim, S. Emr, and R. Tsien (personal communication) have found that GFP expression in *Saccharomyces cerevisiae* can make the cells strongly fluorescent without causing toxicity. S. Wang and T. Hazelrigg (personal communication) have found that both COOH-terminal and NH_2-terminal protein fusions with GFP are fluorescent in *D. melanogaster*. L. Lanini and F. McKeon (personal communication) have expressed a GFP protein fusion in mammalian (COS) cells.
24. We have generated several other plasmid constructions that may be useful to investigators. These include a pBluescript II KS (+) derivative (TU#65) containing a Kpn I–Eco RI fragment encoding GFP with an Age I site 5′ to the translation start and a Bsm I site at the termination codon. Also available are *gfp* versions (TU#60 to TU#63) of the four *C. elegans lacZ* expression vectors (pPD16.43, pPD21.28, pPD22.04, and pPD22.11, respectively) as described (*27*) except that they lack the Kpn I fragment containing the SV40 nuclear localization signal.
25. J. P. Miller and A. Selverston, *Science* **206**, 702 (1979).
26. J. Sanbrook, E. F. Fritsch, T. Maniatis, *Molecular Cloning: A Laboratory Manual* (Cold Spring Harbor Laboratory Press, Cold Spring Harbor, NY, ed. 2, 1989).
27. A. Fire, S. W. Harrison, D. Dixon, *Gene* **93**, 189 (1990).
28. J. C. Way and M. Chalfie, *Cell* **54**, 5 (1988).
29. We are indebted to A. Duggan and D. Xue for technical suggestions, to L. Kerr and P. Presley at the Marine Biological Laboratories at Woods Hole for help with microscopy, to M. Cutler and R. Ludescher for assistance in obtaining the excitation and emission spectra, to A. Fire for suggestions on vector construction, and to the colleagues listed in (*8*) and (*23*) for permission to cite their unpublished research. Supported by NIH grant GM31997 and a McKnight Development Award to M.C. and by American Cancer Society grant NP640 to D.C.P.

15 September 1993; accepted 16 November 1993

RNA Polymerase II Initiation Factor Interactions and Transcription Start Site Selection

Yang Li, Peter M. Flanagan, Herbert Tschochner,* Roger D. Kornberg†

An RNA polymerase II transcription system was resolved and reconstituted from extracts of *Schizosaccharomyces pombe*. Exchange with components of a *Saccharomyces cerevisiae* system was undertaken to reveal the factor or factors responsible for the difference in location of the transcription start site, about 30 base pairs and 40 to 120 base pairs downstream of the TATA box in *S. pombe* and *S. cerevisiae*, respectively. Two components, counterparts of human transcription factor IIF (TFIIF) and TFIIH, could be exchanged individually between systems without effect on the start site. Three components, counterparts of human TFIIB, TFIIE, and RNA polymerase II, could not be exchanged individually but could be swapped in the pairs TFIIE-TFIIH and TFIIB–RNA polymerase II, which demonstrates that there are functional interactions between these components. Moreover, exchange of the latter pair shifted the starting position, which shows that TFIIB and RNA polymerase II are solely responsible for determining the start site of transcription.

Synthesis of mRNA in eukaryotes requires RNA polymerase II and accessory factors, some which are general and act at most, if not all, promoters, and others of which confer specificity and control. Five general factors—a, b, d, e, and g—have been purified to homogeneity from the budding yeast *Saccharomyces cerevisiae* and have been identified as counterparts of human-rat factors TFIIE-ϵ, TFIIH-δ, TFIID-τ, TFIIB-α, and TFIIF-βγ, respectively (*1*–*8*). Because these factors assemble at a promoter in a complex with RNA polymerase II, interactions among them are assumed to be important for the initiation of transcription.

Most studies of general factor interactions have focused on binding (*8*). The results have shown that the order of assembly of the initiation complex on promoter DNA begins with factor d (TFIID), is followed by factor e (TFIIB), and then by polymerase and the remaining factors (6, 9). Factors b (TFIIH), e, and g (TFIIF), however, bind directly to polymerase II, and as many as four of the five factors may assemble with the polymerase in a holoenzyme (*10*) before promoter binding. There are a couple of limitations implicit in these findings: The functional significance of interactions revealed by binding is questionable because only a few percent of initiation complexes give rise to transcripts, and there is little indication of the roles of the various interactions in the initiation process.

We have used a functional approach to analyze general transcription factor interactions on the basis of the ability of factors to be exchanged between transcription systems. Exchange between *S. cerevisiae* and mammalian systems is of interest because of a marked difference in location of the transcription start site, 40 to 120 base pairs downstream of the TATA box in the former versus about 30 base pairs in the latter (*11*). The TATA-binding component (TBP) of factor d (TFIID) is functionally interchangeable between *S. cerevisiae* and humans (*4*, *12*, *13*), but the transcription start site remains characteristic of the particular transcription system, irrespective of the source of TBP. The factor or factors responsible for start site selection could not be identified by this approach because neither the other factors nor the polymerase proved interchangeable between *S. cerevisiae* and higher eukaryotic systems. We decided to use a *Schizosaccharomyces pombe* system because of its similarity to higher eukaryotes in the location of RNA polymerase II transcription start sites and its closer evolutionary relation to *S. cerevisiae*. Initiation from *S. pombe* promoters occurs about 30 base pairs downstream of the TATA box, and initiation from mammalian promoters introduced in *S. pombe* occurs at the same sites as in mammalian cells (*14*).

We have described the derivation of a chromatographic fraction from *S. pombe* that, upon addition of TBP, will support promoter-dependent RNA polymerase II transcription

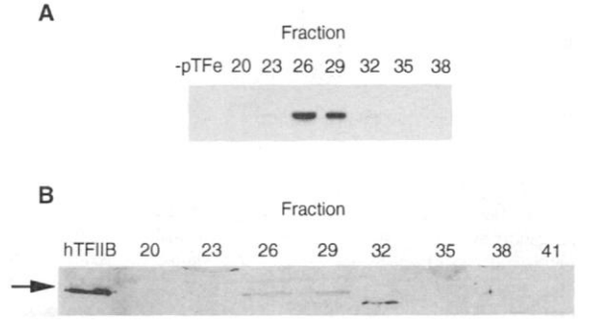

Fig. 1. Factor e of *S. pombe* copurifies with a 35-kD polypeptide cross-reactive with human TFIIB antiserum. (**A**) Assay of fractions (2 μl) from HAP (*16*) for pTFe activity. Assays were performed with the complete *S. pombe* system (*16*), except for the omission (first lane) of pTFe. (**B**) Immunoblot analysis of fractions (40 μl) from HAP. Trichloroacetic acid precipitation, 12% SDS–polyacrylamide gel electrophoresis, and blotting onto nitrocellulose were followed by successive incubations with polyclonal human TFIIB antiserum (1:300) for 18 hours at 4°C and with goat monoclonal antibody to rabbit (1:2000) for 1 hour at 24°C as described (*26*). The 35-kD polypeptide (indicated by arrow) was the only cross-reactive species seen when smaller amounts of protein were loaded. Lane 1 contained 10 ng of human TFIIB.

Department of Cell Biology, Stanford University, School of Medicine, Stanford, CA 94305, USA.

*Present address: Institute fur Biochemie I, Der Universitat Heidelberg, Im Neuenheimer Feld 328, 6900 Heidelberg, Germany.
†To whom correspondence should be addressed.

nature biotechnology

Improved monomeric red, orange and yellow fluorescent proteins derived from *Discosoma* sp. red fluorescent protein

Nathan C Shaner[1], Robert E Campbell[1,6], Paul A Steinbach[1], Ben N G Giepmans[3,4], Amy E Palmer[1] & Roger Y Tsien[1,2,5]

Fluorescent proteins are genetically encoded, easily imaged reporters crucial in biology and biotechnology[1,2]. When a protein is tagged by fusion to a fluorescent protein, interactions between fluorescent proteins can undesirably disturb targeting or function[3]. Unfortunately, all wild-type yellow-to-red fluorescent proteins reported so far are obligately tetrameric and often toxic or disruptive[4,5]. The first true monomer was mRFP1, derived from the *Discosoma* sp. fluorescent protein "DsRed" by directed evolution first to increase the speed of maturation[6], then to break each subunit interface while restoring fluorescence, which cumulatively required 33 substitutions[7]. Although mRFP1 has already proven widely useful, several properties could bear improvement and more colors would be welcome. We report the next generation of monomers. The latest red version matures more completely, is more tolerant of N-terminal fusions and is over tenfold more photostable than mRFP1. Three monomers with distinguishable hues from yellow-orange to red-orange have higher quantum efficiencies.

Although mRFP1 overcame DsRed's tetramerization and sluggish maturation and exceeded DsRed's excitation and emission wavelengths by about 25 nm, the extinction coefficient, fluorescence quantum yield and photostability decreased somewhat during its evolution[7]. To minimize these sacrifices, we subjected mRFP1 to many rounds of directed evolution using both manual and fluorescence-activated cell sorting (FACS)-based screening. The properties of the resulting variants include several new colors, increased tolerance of N- and C-terminal fusions, and improvements in extinction coefficients, quantum yields and photostability, although no single variant is optimal by all criteria.

The red chromophore of DsRed results from the autonomous multi-step post-translational modification of residues Gln66, Tyr67 and Gly68 into an imidazolidinone heterocycle with *p*-hydroxybenzylidene and acylimine substituents[8]. Our first attempt at improving the brightness of mRFP1 involved construction of a directed library in which residues near the chromophore, including position 66, were randomized. The top clone of this library, mRFP1.1, contains the mutation Q66M, which promotes more complete maturation and provides an additional 5 nm red-shift of both the excitation and emission spectra relative to mRFP1. We then set out to reduce the sensitivity of mRFP1.1 to N-terminal fusions. Because *Aequorea victoria* green fluorescent protein (GFP) is relatively indifferent to N- or C-terminal fusions, we eventually generated mRFP1.3 by replacing the first seven amino acids of mRFP1.1 with the corresponding residues from enhanced GFP (MVSKGEE) followed by a spacer sequence NNMA (numbered 6a–d), and appending the last seven amino acids of GFP to the C terminus. mRFP1.3, unlike its predecessors, was found to have an equivalent high level of fluorescence regardless of fusions to its N terminus.

Through additional rounds of screening random libraries based on mRFP1.3 and wavelength-shifted mRFP variants, we identified the beneficial folding mutations V7I and M182K, which were incorporated into clone mRFP1.4. Randomization of position 163 in mRFP1.4 led to the identification of the substitution M163Q, which results in a nearly complete disappearance of the absorbance peak at ~510 nm, present in all previous mRFP clones. The additional mutations N6aD, R17H, K194N, T195V and D196N were introduced through two further rounds of directed evolution to produce our final optimized clone, mCherry (**Table 1** and **Figs. 1**, **2** and **3**).

To test whether the introduction of GFP-type termini into mRFP variants would benefit fusion proteins expressed in mammalian cells, we fused mRFP1 and mCherry to the N terminus of α-tubulin. In most HeLa cells, expression of mRFP1-α-tubulin resulted in diffuse cytoplasmic fluorescence rather than proper incorporation into microtubules (**Fig. 3b**). However, mCherry-α-tubulin fusions were successfully incorporated into microtubules in most cells (**Fig. 3c**), similar to results seen with GFP-coupled tubulin[9]. The amount of full-length mRFP1-α-tubulin expressed was similar to that of mCherry-α-tubulin as verified by in-gel fluorescence and western blot analysis (data not shown). Equivalent results were obtained with Madin-Darby canine kidney and primary human fibroblasts (data not shown). By

[1]Departments of Pharmacology, [2]Chemistry and Biochemistry, and [3]Neurosciences, [4]National Center of Microscopy and Imaging Research, and [5]Howard Hughes Medical Institute, University of California at San Diego, 9500 Gilman Drive, La Jolla, California 92093, USA. [6]Present address: Department of Chemistry, University of Alberta, Edmonton, Alberta T6G 2G2, Canada. Correspondence should be addressed to (rtsien@ucsd.edu).

Published online 21 November 2004; doi:10.1038/nbt1037

Table 1 Properties of novel fluorescent protein variants

Fluorescent protein	Excitation maximum (nm)	Emission maximum (nm)	Extinction coefficient per chain[a] ($M^{-1}cm^{-1}$)	Fluorescence quantum yield	Brightness of fully mature protein (% of DsRed)	pKa	$t_{0.5}$ for maturation at 37 °C	$t_{0.5}$ for bleach[b], s
DsRed	558	583	75,000	0.79	100	4.7	~10 h	ND
T1	555	584	38,000	0.51	33	4.8	<1 h	ND
Dimer2	552	579	69,000	0.69	80	4.9	~2 h	ND
mRFP1	584	607	50,000	0.25	21	4.5	<1 h	6.2
mHoneydew	487/504	537/562	17,000	0.12	3	<4.0	ND	5.9
mBanana	540	553	6,000	0.70	7	6.7	1 h	1.4
mOrange	548	562	71,000	0.69	83	6.5	2.5 h	6.4
dTomato	554	581	69,000	0.69	80	4.7	1 h	64
tdTomato	554	581	138,000	0.69	160	4.7	1 h	70
mTangerine	568	585	38,000	0.30	19	5.7	ND	5.1
mStrawberry	574	596	90,000	0.29	44	<4.5	50 min	11
mCherry	587	610	72,000	0.22	27	<4.5	15 min	68

[a]Extinction coefficients were measured by the alkali denaturation method[8,30] and are believed to be more accurate than the previously reported values for DsRed, T1, dimer2 and mRFP1[7]. [b]Time (s) to bleach to 50% emission intensity, at an illumination level that causes each molecule to emit 1,000 photons/s initially, that is, before any bleaching has occurred. See Methods for more details. For comparison, the value for EGFP is 115 s, assuming an extinction coefficient of 56,000 $M^{-1}cm^{-1}$ and quantum efficiency of 0.60 (ref. 30). ND, not determined.

contrast, fusions of β-actin with mRFP1 or mCherry were both successfully incorporated into the actin cytoskeleton (data not shown).

The dimer2 variant previously described[7] possesses many desirable properties, such as a faster and more complete maturation than wild-type DsRed and a greater fluorescent brightness than the fast-maturing mutant T1 (ref. 6) (DsRed-Express). Through five rounds of directed evolution, we found the optimal combination of mutations to be V22M, Q66M, V105L and F124M, which resulted in improved maturation kinetics, a substantially reduced 'dead-end' green component and a small red-shift. The final clone, designated dimer (d)Tomato (**Table 1** and **Figs. 1** and **2b**), contains GFP-type termini similar to those of mCherry, which result in a higher tolerance of N- and C-terminal fusions (data not shown). To construct a non-aggregating tag from the extremely bright dTomato, we genetically

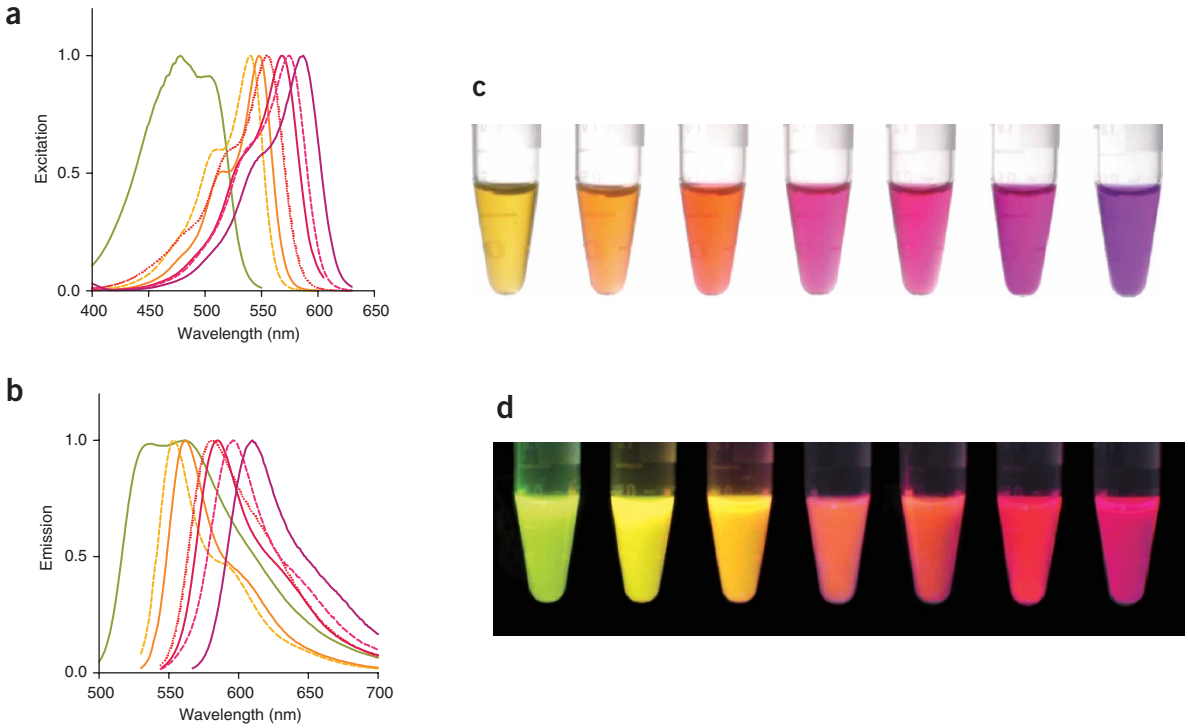

Figure 1 Excitation and emission spectra for new RFP variants. Spectra are normalized to the excitation and emission peak for each protein. (**a**,**b**) Excitation (**a**) and emission (**b**) curves are shown as solid or dashed lines for monomeric variants and as a dotted line for dTomato and tdTomato, with colors corresponding to the color of each variant. (**c**,**d**) Purified proteins (from left to right, mHoneydew, mBanana, mOrange, tdTomato, mTangerine, mStrawberry, and mCherry) are shown in visible light (**c**) and fluorescence (**d**). The fluorescence image is a composite of several images with excitation ranging from 480 nm to 560 nm.

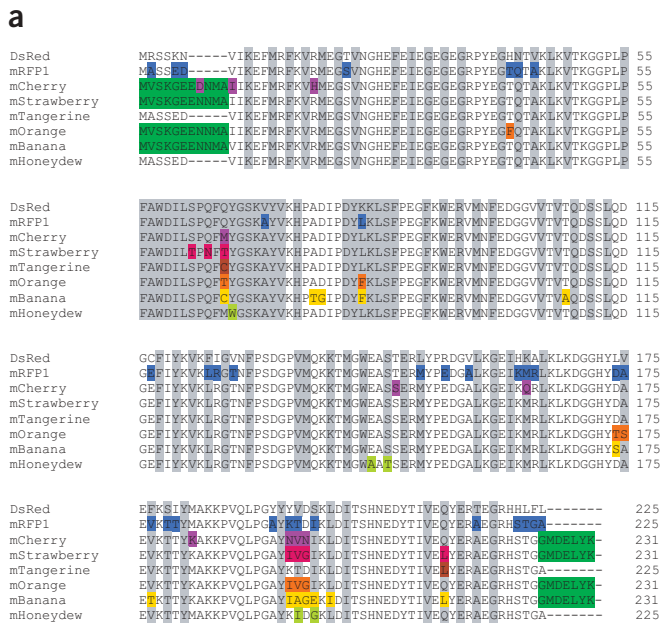

Figure 2 Sequences and genealogy. (**a**) Sequence alignment of mRFP variants with wild-type DsRed and mRFP1. Internal residues are shaded. mRFP1 mutations are shown in blue, and critical mutations in mCherry, mStrawberry, mTangerine, mOrange, mBanana and mHoneydew are shown in colors corresponding to the color of each variant. GFP-type termini on mRFP variants are shown in green. (**b**) A genealogy of DsRed-derived variants, with mutations critical to the phenotype of each variant. GenBank accession numbers are given under the name of each variant.

fused two copies of the gene to create a tandem dimer (td), as previously reported[7] (see Methods).

Many new fluorescent proteins with different colors have been discovered in diverse anthozoan species, but so far they all suffer from obligate tetramerization and would require efforts similar to the evolution of mRFP1 to produce widely useful fusion partners[10]. Because such monomerization is usually tedious and often unsuccessful, it might be more efficient to alter the excitation and emission wavelength of mRFP through directed evolution. Following the example of GFP engineering[11,12], we explored substitutions at Gln66 and Tyr67, homologous to Tyr66 and Ser65 in GFP (see **Supplementary Notes** online for details on the variants mHoneydew (Y67W) and mBanana (Q66C, I197E)).

Initial mutations of position 66 in mRFP1.1 indicated that the substitutions Q66S, Q66T, and Q66C all yielded proteins substantially blue-shifted with respect to mRFP1. This led us to the development of mTangerine, which contains the substitutions Q66C and Q213L with respect to mRFP1.1 (**Fig. 2**), with excitation and emission peaks at 568 and 585 nm (**Fig. 1**). Although mTangerine has a respectable extinction coefficient (38,000 $M^{-1}cm^{-1}$) and quantum yield (0.3), we quickly moved on to development of Gln66-substituted mutants of mRFP1.4, with its optimized N and C termini.

Six rounds of directed evolution of mRFP1.4 M66T produced the final orange fluorescent variant, mOrange, with excitation and emission peaks at 548 nm and 562 nm (**Table 1** and **Figs. 1** and **2**), similar to those of a tetrameric orange fluorescent protein from *Cerianthus* sp.[13] and a monomer evolved from a *Fulgia concinna* fluorescent protein[14]. mOrange has an extinction coefficient equivalent to that of mCherry, but a more than threefold higher quantum yield. Though mOrange is the brightest true monomer in the present series, it does exhibit substantial acid sensitivity, with a pKa of 6.5. However, the popular *A. victoria* GFP variant enhanced yellow fluorescent protein, with a pKa of 7.1 (ref. 15), has been used successfully as a qualitative fusion tag by many researchers. Additionally, from the initial mRFP1.4 M66T clone, through five rounds of directed evolution, we created a pH-stable orange-red variant, mStrawberry, which has the highest extinction coefficient (90,000 $M^{-1}cm^{-1}$) of the true monomers. Its wavelengths (excitation 574 nm, emission 596 nm) and quantum yield (0.29) are intermediate between those of mCherry and mOrange (**Table 1** and **Figs. 1** and **2**).

The high extinction coefficient and quantum yield of mOrange made it attractive as a potential fluorescence resonance energy transfer (FRET) acceptor for GFP variants. To test this possibility, we constructed a Zn^{2+} sensor with mOrange and the violet-excited GFP mutant T-Sapphire[16] and compared it to the same sensor containing cyan fluorescent protein (CFP) and the citrine[17] variety of YFP. T-Sapphire was chosen as the donor because it is optimally excited below 425 nm, where mOrange is negligibly excited. The domain that changes its conformation upon binding Zn^{2+} was modified from the original zif-268-derived version[18] by mutating the two Zn^{2+}-binding cysteines to histidine to eliminate any possibility of oxidation. The fusion of CFP and citrine respectively to the N and C termini of the modified Zn^{2+} finger displayed a 5.2-fold ratio change upon addition of Zn^{2+}, with an apparent K_d of ~200 μM. The corresponding mOrange-T-Sapphire combination yielded a sensor whose 562- to 514-nm emission ratio increased sixfold upon Zn^{2+}

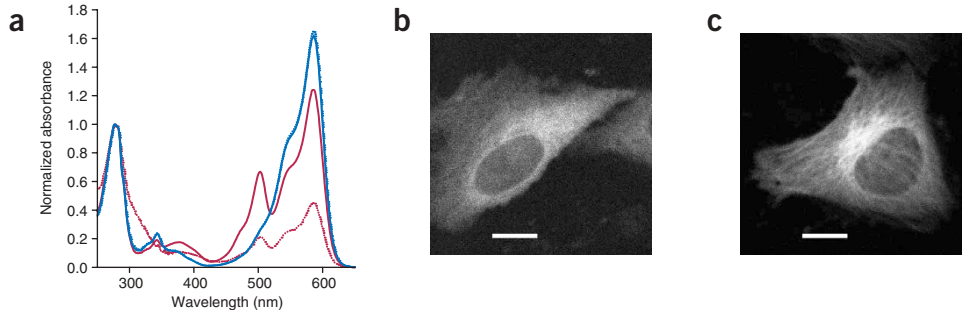

Figure 3 mCherry performance in fusion constructs. (**a**) mCherry is less sensitive than mRFP1 to the presence versus absence of an N-terminal fusion. mRFP1 and mCherry with N-terminal leader sequence containing a 6× His tag (derived from pRSET$_B$) or C-terminal tail with Myc-tag and 6× His tag (derived from pBAD-Myc-His-A (Invitrogen)) were purified on Ni-NTA agarose beads in parallel with extensive washes. Absorbance spectra were taken and normalized to the 280 nm peak for each. Absorbance curves for mRFP1 are plotted in red, and those from mCherry are plotted in blue. Solid lines correspond to N-terminal 6× His-tagged protein, and dotted lines correspond to C-terminal 6× His-tagged protein. Whereas mRFP1 exhibited greatly reduced expression and apparent extinction coefficient (approximately fourfold lower) when expressed with the C-terminal tag, mCherry produced nearly identical results with either N-terminal or C-terminal tags. (**b**,**c**) Expressed in HeLa cells by transient transfection, mRFP1-α-tubulin (**b**) fails to incorporate into microtubules, whereas mCherry-α-tubulin (**c**) is incorporated into microtubules, as has been shown before for *A. victoria*-derived fluorescent proteins[9]. The mRFP1-α-tubulin image (**b**) was brightened by a factor of 2.5 to enable comparison with the mCherry-α-tubulin image (**c**). Microtubules containing mCherry-α-tubulin display dynamic behavior as expected for functional microtubules (data not shown). Scale bars, 10 μm.

binding (**Supplementary Fig. 1** online). This demonstrates that mOrange and T-Sapphire make a good emission-ratiometric FRET pair with a dynamic range at least equaling CFP and YFP but at longer emission wavelengths.

What is the basis of the spectral shifts of these mRFP variants? The largest single effect is seen with substitutions at chromophore position 66, where substitution with serine, threonine or cysteine results in a substantial blue-shift. In the absence of compensating mutations, the Q66S/T/C variants of mRFP1 all exhibit emission around 580 nm at neutral pH, but become brighter and more blue-shifted at high pH. The blue-shifted (mOrange) species is stabilized by T41F and L83F mutations, whereas the red-shifted (mStrawberry) form is favored by S62T, Q64N and Q213L. In mBanana (see **Supplementary Notes** online), the I197E mutation may contribute a hydrogen bond between the glutamate side chain and phenolate oxygen in the chromophore, resulting in a further redistribution of electron density. Confirmation or more detailed explanations await high-resolution structural information.

An obvious application of the proliferation of fluorescent protein colors is to discriminate many cell types, transcriptional activities or fusion proteins. In the most general case, determination of the n independent concentrations of each of the fluorescent proteins requires spectral or lifetime unmixing of at least n measurements. Such unmixing techniques have been shown to discriminate fluorescent species having spectra even more closely overlapping than the current palette[19,20]. However, there is an important special case where each cell or nonoverlapping subcellular structure has been tagged with a different fluorescent protein. When a cell or voxel contains at most one fluorescent protein, how many measurements are required to decide its identity and concentration? To determine this, bacteria separately transfected with EGFP, citrine, mBanana, mOrange, mStrawberry or mCherry were mixed and analyzed by flow cytometry, with excitation at 514 nm and emission simultaneously measured through three bandpass filters, 540–560 nm, 564–606 nm and 595–635 nm. Transformation of the three signals to polar coordinates enabled easy discrimination of the six populations and the relative amounts of fluorescent protein per cell (**Supplementary Fig. 2** online). Thus three simple emission measurements are sufficient.

We compared the photostability of mRFP1 with that of its descendants and of EGFP (see Methods). To make fair comparisons among proteins with different extinction coefficients, overlaps with excitation filters and quantum yields, we normalized the bleach rates to an initial emission rate from each molecule of 1,000 photons/s. The resulting bleach curves (**Supplementary Fig. 3** online) varied greatly in absolute rate but were generally far from single exponentials. Most showed an initial fast phase in which over 50% of the initial emission was lost, followed by a lower-amplitude, much slower decay phase. This complexity makes it difficult to extract a meaningful single number for the quantum efficiency of photobleaching. Therefore, we believe a realistic figure of merit for typical cell biological experiments is the time for the emission to drop to 50% of its initial value. These values are listed in **Table 1**. By this criterion, the best performers are tdTomato and mCherry, which are both more than tenfold better than mRFP1 and nearly as good as EGFP.

Just as no one type of fruit in a grocery store supplants all others, so there is no single best fluorescent protein within the cornucopia derived from DsRed via mRFP1 and dimer2. The highest brightness (product of extinction coefficient, 138,000 $M^{-1}cm^{-1}$, and quantum yield, 0.69) is found in tdTomato, at the cost of doubling the molecular weight. A previous tandem dimer, t-HcRed1, was reported to have an extinction coefficient and quantum yield of 160,000 $M^{-1}cm^{-1}$ and 0.04 (ref. 21), corresponding to about 15-fold less brightness than that of tdTomato. Among the true monomers, mCherry offers the longest wavelengths, the highest photostability, the fastest maturation and excellent pH resistance. Its excitation and emission maxima are just 3 nm longer than those of mRFP1, for which it is the closest upgrade. Although mCherry's quantum efficiency is slightly lower (0.22 versus 0.25 for mRFP1), its higher extinction coefficient (due to near-complete maturation), tolerance of N-terminal fusions and photostability make mRFP1 obsolete. For applications such as dual-emission FRET in which the acceptor's quantum yield must be maximized, mOrange is the current favorite (e.g., **Supplementary Fig. 1** online), though its maturation time, pH sensitivity and photostability are currently far from optimal. Additional colors for multiwavelength tracking of distinct cells or

substructures are available from mStrawberry, mTangerine, mBanana and mHoneydew in descending order of wavelengths and brightness.

What other possibilities exist for the engineering of mRFP-derived proteins? Other desirable properties that exist in tetrameric fluorescent proteins and their relatives are reversible photoactivation[22], red-to-green photoconversion[23,24] and more extreme red-shifts[10,21,25]. One could also imagine the engineering of other more unconventional properties, such as phosphorescence or generation of singlet oxygen. Monomeric proteins with such properties would be quite valuable. Evolution of such proteins or recombination of the best features of the existing proteins will probably require even higher-throughput means to generate genetic diversity, coupled with new screens run in parallel for all requisite performance criteria.

METHODS

Mutagenesis and screening. mRFP1 and dimer2 (ref. 7) were used as the initial templates for construction of genetic libraries by a combination of saturation or partial saturation mutagenesis at particular residues and random mutagenesis of the whole gene. Random mutagenesis was performed by error-prone PCR as described[17] or by using the GeneMorph I or GeneMorph II kit (Stratagene). Mutations at specific residues were introduced as described[7], or by sequential QuikChange (Stratagene), or by QuikChange Multi (Stratagene) or by a ligation-based method (description follows). Briefly, oligonucleotide primers containing the degenerate codons of interest at their 5′ ends preceded by a *Sap*I restriction site were used to amplify the RFP in two separate PCR reactions using PfuTurbo polymerase (Stratagene). Each PCR fragment was cut with SapI (New England Biolabs) to produce a 3-base overhang compatible with the other digested fragment, and purified digested fragments were ligated with T4 DNA ligase (New England Biolabs). Full-length ligation product inserts were gel purified and digested with EcoRI/BamHI (New England Biolabs) and inserted into $pRSET_B$ or a modified pBAD vector (Invitrogen). For all library construction methods, chemically competent or electrocompetent *Escherichia coli* strain JM109(DE3) (for $pRSET_B$) or LMG194 (for pBAD)[26] were transformed and grown overnight on LB/agar (supplemented with 0.02% (wt/vol) L-arabinose (Fluka) for pBAD constructs) at 37 °C and maintained thereafter at 25 °C. Luria-Bertani (LB)/agar plates were manually screened as previously described[27]. JM109(DE3) colonies of interest were cultured overnight in 2 ml LB supplemented with ampicillin. LMG194 colonies of interest were cultured for 8 h in 2 ml minimal medium (RM) supplemented with ampicillin and 0.2% (wt/vol) D-glucose, and then culture volume was increased to 4 ml with LB/ampicillin. RFP expression was then induced by adding L-arabinose to a final concentration of 0.2% (wt/vol) and cultures were allowed to continue growing overnight. For both JM109(DE3) and LMG194, a fraction of the cell pellet was extracted with B-PER II (Pierce), and spectra were obtained using a Safire 96-well plate reader with monochromators (TECAN). DNA was purified from the remaining pellet by QIAprep spin column (Qiagen) and submitted for sequencing.

Construction of tandem dimer and FRET constructs. To construct tdTomato with a 12-residue linker (GHGTGSTGSGSS), dTomato was amplified in two separate PCR reactions, the first PCR retaining the 7-residue GFP-type N terminus (MVSKGEE) but deleting the 7-residue GFP-type C terminus and adding the first half of the 12-residue linker followed by a *Sap*I restriction site, and the second PCR adding the remaining half of the 12-residue linker followed by the sequence ASSEDNNMA before residue 7 of dTomato, and ending with the 7-residue GFP-type C terminus (GMDELYK). Agarose gel-purified PCR products were digested with *Sap*I, gel purified and ligated with T4 DNA ligase. The full-length ligation product was gel purified, digested with *Eco*RI/*Bam*HI and ligated into a modified pBAD vector. For FRET constructs, the original Zn^{2+} sensor[18] was modified such that the two Zn^{2+}-ligating cysteine residues were mutated to histidine. The modified Zn^{2+} finger domain, HERPYA**H**PVES**H**DRFSRSDELTR**H**IRI**H**TGQK (Zn^{2+} ligating residues in bold, mutated residues underlined), was inserted between CFP and citrine with *Sph*I and *Sac*I sites as linkers. PCR-amplified mOrange and T-Sapphire[16] were inserted into *Bam*HI/*Sph*I and *Eco*RI/*Sac*I sites, replacing CFP and citrine.

Protein production and characterization. RFPs were expressed from pBAD vectors in *E. coli* LMG194 by growing single colonies in 40 ml RM/ampicillin supplemented with 0.2% D-glucose for 8 h, adding 40 ml LB/ampicillin and L-arabinose to a final concentration of 0.2%, and incubating overnight at 37 °C. For maturation experiments, flasks were sealed with parafilm upon induction to restrict oxygen availability. All proteins were purified by Ni-NTA chromatography (Qiagen) and dialyzed into PBS. Biochemical and fluorescence characterization experiments were done as described[5]. For FRET measurements, purified Zn^{2+} sensor proteins were diluted in 10 mM MOPS, 100 mM KCl, pH 7.4 with either 1 mM EDTA or 1 mM $ZnCl_2$, and fluorescence emission spectra were collected with excitation near the peak donor excitation wavelength.

Cloning of tubulin chimeras, transfection and imaging. cDNAs were inserted following standard procedures into the *Hin*dIII and *Xho*I sites of pCDNA3.1 (Invitrogen), resulting in cDNAs encoding mRFP1-GGR-human-α-tubulin and mCherry-SGLRSRA-human-α-tubulin, both lacking the first methionine of tubulin. PCR-mediated cloning was verified by automated sequencing. HeLa cells were grown in 3-cm dishes with poly-D-lysine coated glass-bottoms (Matek) in DMEM supplemented with penicillin and streptomycin and 10% fetal calf serum. HeLa cells were transfected using Fugene (Invitrogen) and analyzed 2 d post-transfection. Imaging was done on a Biorad MRC1024 confocal system, controlled by Lasersharp2000 software. The stage was maintained at 37 °C using a lens heater (Bioptechs) and a 3-cm water-circulation-based dish heater. Acquisition was in one focal plane, using 568 nm excitation and collecting >585 nm emission.

Electrophoresis, in-gel fluorescence and western blot analysis. Transfected cells were lysed in 120 µl Laemmli Sample Buffer (50 mM Tris pH 6.8, 2% (wt/vol) SDS, 10% (vol/vol) glycerol, 5% (vol/vol) β-mercaptoethanol, 0.1% (wt/vol) bromophenol blue) and the lysates were sheared. Lysates were either left untreated (in-gel fluorescence assay) or heated for 10 min at 95 °C (western blot). We ran 15 µl of each sample on a 10–20% Novex Tris-Glycine gel (Invitrogen). Fluorescence was measured using 560/40 nm excitation and 620/20 nm emission filters. The gel with the denaturated samples was transferred to Immobilon (Millipore). The membranes were blocked in 2.5% (wt/vol) BSA and subsequently probed with primary antibody anti-α-tubulin (B512, Sigma) followed by goat-anti-mouse antibody conjugated to horseradish peroxidase (Calbiochem). Blots were washed extensively, and immunostained proteins were visualized using Western Lightning Chemiluminescence (Perkin Elmer).

FACS. A modified version of the protocol described[28] was used for FACS screening of large libraries of fluorescent protein mutants. Briefly, *E. coli* LMG194 was electroporated with a modified pBAD vector containing the gene library, and the transformed cells were grown in 30 ml RM supplemented with ampicillin and 0.2% (wt/vol) D-glucose. After 8 h, RFP expression was induced by adding L-arabinose to a final concentration of 0.2% (wt/vol). Cultures induced overnight were diluted 1:100 into Dulbecco's PBS supplemented with ampicillin before FACS sorting. Multiple rounds of cell sorting were done on a FACSDiva (BD Biosciences) in yield-mode for the first sort and purity- or single-cell mode for subsequent sorts of the same library. Sorted cells were grown overnight in 4 ml RM/amp with 0.2% (wt/vol) D-glucose and the resulting saturated culture was diluted 1:100 into 30 ml RM/Amp with 0.2% (wt/vol) D-glucose to start the next culture to be sorted. After three to four rounds of FACS sorting, the bacteria were plated onto LB/agar supplemented with 0.02% (wt/vol) L-arabinose and grown overnight, after which individual clones were screened manually as described above.

Photobleaching measurements. Aqueous droplets of purified protein in PBS were formed under mineral oil in a chamber on the fluorescence microscope stage. For reproducible results it proved essential to pre-extract the oil with aqueous buffer, which would remove any traces of autoxidized or acidic contaminants. The droplets were small enough (5–10 µm diameter) so that all the molecules would see the same incident intensity. The absolute excitation irradiance in photons/($cm^2 \times s \times nm$) as a function of wavelength was computed from the spectra of a xenon lamp, the transmission of the excitation filter, the reflectance of the dichroic mirror, the manufacturer-supplied absolute spectral sensitivity of a miniature integrating-sphere detector (SPD024 head and ILC1700 meter, International Light Corp.) and the measured detector current.

The predicted rate of initial photon emission per chromophore (before any photobleaching had occurred) was calculated from the excitation irradiance and absorbance spectrum (both as functions of wavelength), and the quantum yield. These rates varied from 180 s^{-1} for mHoneydew to 3,300 s^{-1} for mStrawberry. To normalize the observed photobleaching time courses to a common arbitrary standard of 1,000 emitted photons/s, the time axes were correspondingly scaled by factors of 0.18 to 3.3, assuming that emission and photobleach rates are both proportional to excitation intensity at intensities typical of microscopes with arc lamp sources, as is known to be the case for GFP[29].

Note: Supplementary information is available on the Nature Biotechnology website.

ACKNOWLEDGMENTS

All sequences have been deposited in GenBank, accession numbers AY678264 through AY678271. We thank Oliver Griesbeck for the kind donation of T-Sapphire, Coyt Jackson for FACS support, Brent Martin for α-tubulin cDNA, and Rene Meijer and Lei Wang for helpful discussion. Sequencing services were provided by the UCSD Cancer Center shared sequencing resource. N.C.S. is a Howard Hughes Medical Institute Predoctoral Fellow. Construction of tubulin fusions and mammalian cell imaging were conducted at the National Center for Microscopy and Imaging Research, which is supported by National Institutes of Health (NIH) grant RR04050 (to Mark H. Ellisman). This work was also supported by NIH and Department of Energy grants NS27177 and DE-FG-01ER63276.

COMPETING INTERESTS STATEMENT

The authors declare that they have no competing financial interests.

Received 7 July; accepted 5 October 2004
Published online at http://www.nature.com/naturebiotechnology/

1. Tsien, R.Y. The green fluorescent protein. *Annu. Rev. Biochem.* **67**, 509–544 (1998).
2. Zhang, J., Campbell, R.E., Ting, A.Y. & Tsien, R.Y. Creating new fluorescent probes for cell biology. *Nat. Rev. Mol. Cell Biol.* **3**, 906–918 (2002).
3. Lauf, U., Lopez, P. & Falk, M.M. Expression of fluorescently tagged connexins: a novel approach to rescue function of oligomeric DsRed-tagged proteins. *FEBS Lett.* **498**, 11–15 (2001).
4. Matz, M.V. *et al.* Fluorescent proteins from nonbioluminescent Anthozoa species. *Nat. Biotechnol.* **17**, 969–973 (1999).
5. Baird, G.S., Zacharias, D.A. & Tsien, R.Y. Biochemistry, mutagenesis, and oligomerization of DsRed, a red fluorescent protein from coral. *Proc. Natl. Acad. Sci. USA* **97**, 11984–11989 (2000).
6. Bevis, B.J. & Glick, B.S. Rapidly maturing variants of the *Discosoma* red fluorescent protein (DsRed). *Nat. Biotechnol.* **20**, 83–87 (2002).
7. Campbell, R.E. *et al.* A monomeric red fluorescent protein. *Proc. Natl. Acad. Sci. USA* **99**, 7877–7882 (2002).
8. Gross, L.A., Baird, G.S., Hoffman, R.C., Baldridge, K.K. & Tsien, R.Y. The structure of the chromophore within DsRed, a red fluorescent protein from coral. *Proc. Natl. Acad. Sci. USA* **97**, 11990–11995 (2000).
9. Rusan, N.M., Fagerstrom, C.J., Yvon, A.M. & Wadsworth, P. Cell cycle-dependent changes in microtubule dynamics in living cells expressing green fluorescent protein-alpha tubulin. *Mol. Biol. Cell* **12**, 971–980 (2001).
10. Verkhusha, V.V. & Lukyanov, K.A. The molecular properties and applications of Anthozoa fluorescent proteins and chromoproteins. *Nat. Biotechnol.* **22**, 289–296 (2004).
11. Heim, R., Cubitt, A.B. & Tsien, R.Y. Improved green fluorescence. *Nature* **373**, 663–664 (1995).
12. Heim, R., Prasher, D.C. & Tsien, R.Y. Wavelength mutations and posttranslational autoxidation of green fluorescent protein. *Proc. Natl. Acad. Sci. USA* **91**, 12501–12504 (1994).
13. Ip, D.T. *et al.* Crystallization and preliminary crystallographic analysis of a novel orange fluorescent protein from the Cnidaria tube anemone *Cerianthus* sp. *Acta Crystallogr. D Biol. Crystallogr.* **60**, 340–341 (2004).
14. Karasawa, S., Araki, T., Nagai, T., Mizuno, H. & Miyawaki, A. Cyan-emitting and orange-emitting fluorescent proteins as a donor/acceptor pair for fluorescence resonance energy transfer. *Biochem. J.* **381**, 307–312 (2004).
15. Llopis, J., McCaffery, J.M., Miyawaki, A., Farquhar, M.G. & Tsien, R.Y. Measurement of cytosolic, mitochondrial, and Golgi pH in single living cells with green fluorescent proteins. *Proc. Natl. Acad. Sci. USA* **95**, 6803–6808 (1998).
16. Zapata-Hommer, O. & Griesbeck, O. Efficiently folding and circularly permuted variants of the Sapphire mutant of GFP. *BMC Biotechnol.* **3**, 5 (2003). (http://www.biomedcentral.com/1472-6750/3/5).
17. Griesbeck, O., Baird, G.S., Campbell, R.E., Zacharias, D.A. & Tsien, R.Y. Reducing the environmental sensitivity of yellow fluorescent protein. Mechanism and applications. *J. Biol. Chem.* **276**, 29188–29194 (2001).
18. Miyawaki, A. & Tsien, R.Y. Monitoring protein conformations and interactions by fluorescence resonance energy transfer between mutants of green fluorescent protein. *Methods Enzymol.* **327**, 472–500 (2000).
19. Hadjantonakis, A.K., Dickinson, M.E., Fraser, S.E. & Papaioannou, V.E. Technicolour transgenics: imaging tools for functional genomics in the mouse. *Nat. Rev. Genet.* **4**, 613–625 (2003).
20. Farkas, D.L. *et al.* Non-invasive image acquisition and advanced processing in optical bioimaging. *Comput. Med. Imaging Graph.* **22**, 89–102 (1998).
21. Fradkov, A.F. *et al.* Far-red fluorescent tag for protein labelling. *Biochem. J.* **368**, 17–21 (2002).
22. Chudakov, D.M. *et al.* Kindling fluorescent proteins for precise *in vivo* photolabeling. *Nat. Biotechnol.* **21**, 191–194 (2003).
23. Mizuno, H. *et al.* Photo-induced peptide cleavage in the green-to-red conversion of a fluorescent protein. *Mol. Cell* **12**, 1051–1058 (2003).
24. Ando, R., Hama, H., Yamamoto-Hino, M., Mizuno, H. & Miyawaki, A. An optical marker based on the UV-induced green-to-red photoconversion of a fluorescent protein. *Proc. Natl. Acad. Sci. USA* **99**, 12651–12656 (2002).
25. Petersen, J. *et al.* The 2.0-A crystal structure of eqFP611, a far red fluorescent protein from the sea anemone *Entacmaea quadricolor*. *J. Biol. Chem.* **278**, 44626–44631 (2003).
26. Guzman, L.M., Belin, D., Carson, M.J. & Beckwith, J. Tight regulation, modulation, and high-level expression by vectors containing the arabinose PBAD promoter. *J. Bacteriol.* **177**, 4121–4130 (1995).
27. Baird, G.S., Zacharias, D.A. & Tsien, R.Y. Circular permutation and receptor insertion within green fluorescent proteins. *Proc. Natl. Acad. Sci. USA* **96**, 11241–11246 (1999).
28. Daugherty, P.S., Olsen, M.J., Iverson, B.L. & Georgiou, G. Development of an optimized expression system for the screening of antibody libraries displayed on the *Escherichia coli* surface. *Protein Eng.* **12**, 613–621 (1999).
29. Chiu, C.S., Kartalov, E., Unger, M., Quake, S. & Lester, H.A. Single-molecule measurements calibrate green fluorescent protein surface densities on transparent beads for use with 'knock-in' animals and other expression systems. *J. Neurosci. Methods* **105**, 55–63 (2001).
30. Ward, W.W. Biochemical and physical properties of GFP. in *Green Fluorescent Protein: Properties, Applications, and Protocols* (eds. Chalfie, M. & Kain, S.) 45–75 (Wiley, New York, 1998).

8 October 2008

KUNGL. VETENSKAPSAKADEMIEN
THE ROYAL SWEDISH ACADEMY OF SCIENCES

Supporting Document
Not mandatory read past this point

Scientific Background on the Nobel Prize in Chemistry 2008

The green fluorescent protein: discovery, expression and development

The Royal Swedish Academy of Sciences, Information Department, Box 50005, SE-104 05 Stockholm, Sweden
Phone: +46 8 673 95 00, Fax: +46 8 15 56 70, info@kva.se, www.kva.se

Background

During the 20th century the foundations of biochemistry were laid and used to explore the basal principles of the anabolic and catabolic pathways inside living cells. The 20th century also witnessed a revolution in our understanding of enzyme function and, through crystallography and nuclear magnetic resonance, of protein structures revealed at atomic resolution. During the second half of that century, classical genetics and nucleic-acid chemistry merged into modern genomics, based on whole-genome sequencing of an ever increasing number of organisms. This genetics revolution, supported by bioinformatics and other auxiliary techniques, has had an impact in many areas of the biological sciences, with practical consequences for medicine, pharmacy and ecology. However, neither the biochemical nor the genetics revolution provided the experimental tools that would allow for quantitative and experimentally well-defined monitoring at the molecular level of the spatio-temporal intra- and inter-cellular processes that define the dynamic behaviour of all living systems. To obtain such knowledge, new experimental and conceptual tools were required. Now, at the beginning of the 21st century, we are witnessing the rapid development of such tools based on the green fluorescent protein (GFP) from the jellyfish *Aequorea victoria*, its siblings from other organisms and engineered variants of members of the "GFP family" of proteins.

These GFP-like proteins allow the monitoring in time and space of an ever-increasing number of phenomena in living cells and organisms like gene expression, protein localization and dynamics, protein-protein interactions, cell division, chromosome replication and organization, intracellular transport pathways, organelle inheritance and biogenesis, to name but a few. In addition, the fluorescence from single GFP molecules has made it feasible to image at a spatial resolution higher than the diffraction limit. Furthermore, sensors that report pH values, Ca^{2+} concentrations and other essential features of the interior of living cells have been engineered from GFP-like proteins.

The technical revolution resulting from the discovery of GFP relates to a miraculous property of the chromophore that is responsible for its fluorescence. This chromophore is formed spontaneously from a tri-peptide motif in the primary structure of GFP, so that its fluorescence is "automatically" turned on in every organism where it is expressed. In other words, the maturation of the tri-peptide-based chromophore in GFP only requires oxygen and does not depend on the presence of enzymes or other auxiliary factors. GFP and its related variants thereby provide universal genetic tags that can be used to visualize a virtually unlimited number of spatio-temporal processes in virtually all living systems. This GFP revolution in the biological sciences has been greatly accelerated by a rapid parallel development of quantitative light microscopy, electronics, computational power and molecular modelling of intra- and inter-cellular processes with systems-biology approaches.

Outlined below are:(i) basal properties of GFP from *Aequorea victoria*; (ii) basal properties of its native relatives from other organisms and engineered variants of members of the GFP family; (iii) scientific areas in which GFP-like proteins have had a great impact. Then follow three sections of direct relevance for the choice of the Nobel Laureates in 2008: (iv) the discovery of GFP, (v) the demonstration that GFP can fluoresce when expressed in organisms other than *Aequorea victoria*, and (vi) the design of variants of members of the GFP family to create a universal tool-box for the monitoring of spatio-temporal processes in living systems.

Properties of the GFP protein and its fluorescence chromophore

The native green fluorescent protein (GFP), first so named by Morin and Hastings (1971 ab), from the jellyfish *Aequorea victoria* (Shimomura et al., 1962) contains 238 amino acids (Prasher et al., 1992). Residues 65-67 (Ser-Tyr-Gly) in the GFP sequence spontaneously (Heim et al., 1994) form the fluorescent chromophore p-hydroxybenzylideneimidazolinone (Cody et al., 1993; Shimomura, 1979) (Fig. 1).

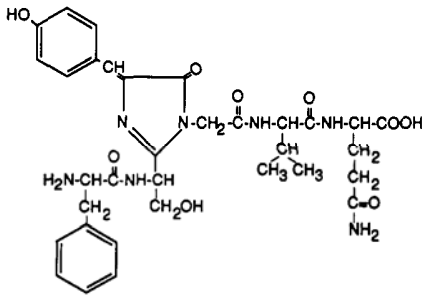

Figure 1. The fluorescence chromophore formed by amino acid residues 65-67 (Ser-Tyr-Gly) in the primary structure of GFP (From Cody et al., 1993).

The excitation spectrum of GFP fluorescence has a dominant maximum at about 400 nm and a significantly smaller maximum at about 470 nm, while the emission spectrum has a sharp maximum at about 505 nm and a shoulder around 540 nm (Tsien, 1998) (Fig. 2).

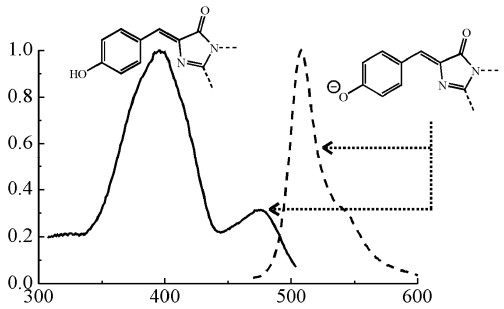

Figure 2. Fluorescence excitation (full-line curve) and emission (dashed curve) spectra of native GFP from *Aequorea victoria* (Tsien et al., 1998).

The crystal structure of GFP (Ormö et al., 1996; Yang et al., 1996) is an eleven-stranded β-barrel, threaded by an α-helix, running up along the axis of the cylinder (Fig. 3). The chromophore (Fig. 1) is in the α-helix, very close to the centre of the can-like cylinder (Fig. 3). A very large part of the primary structure of the protein is used to construct the β-barrel and the threading α-helix. The N-terminal residue and the C-terminal residues 230-238, approximately corresponding to the maximal numbers of residues that can be removed from the N- (2 residues) and C-terminal (6 residues) respectively of GFP at retained fluorescence, are disordered and therefore unresolved in this structural image.

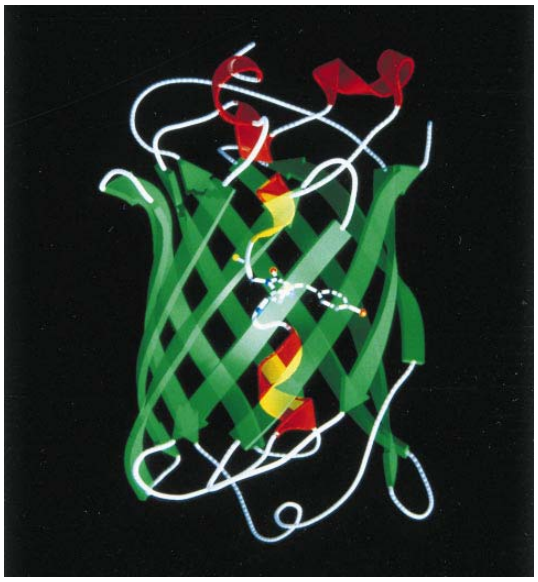

Figure 3. The tertiary structure of GFP, displaying its can-like shape with the α-helix, containing the chromophore, threading up through the can (Brejc et al., 1997).

The tripeptide motif Ser65-Tyr66-Gly67- in the primary structure of unfolded or denatured GFP does not display any striking feature (Fig. 4, top). However, as the GFP protein folds into its native conformation, these three amino acids are forced into a sharp turn (Fig. 4, middle, left), greatly favouring a nucleophilic attack of the amide of Gly67 on the carbonyl of Ser65, leading to imidazolinone formation by cyclization (Fig. 4, middle, right) and dehydration (Fig. 4, bottom, left). At this point, GFP does not fluoresce (Heim et al., 1994) but, conditional on the presence of molecular oxygen, the α–β bond of residue 66 is subsequently dehydrogenated into conjugation with the imidazolinone (Fig. 4, bottom, right), which results in maturation of the GFP chromophore to its fluorescent form (Heim et al., 1994; Cubitt et al., 1995).

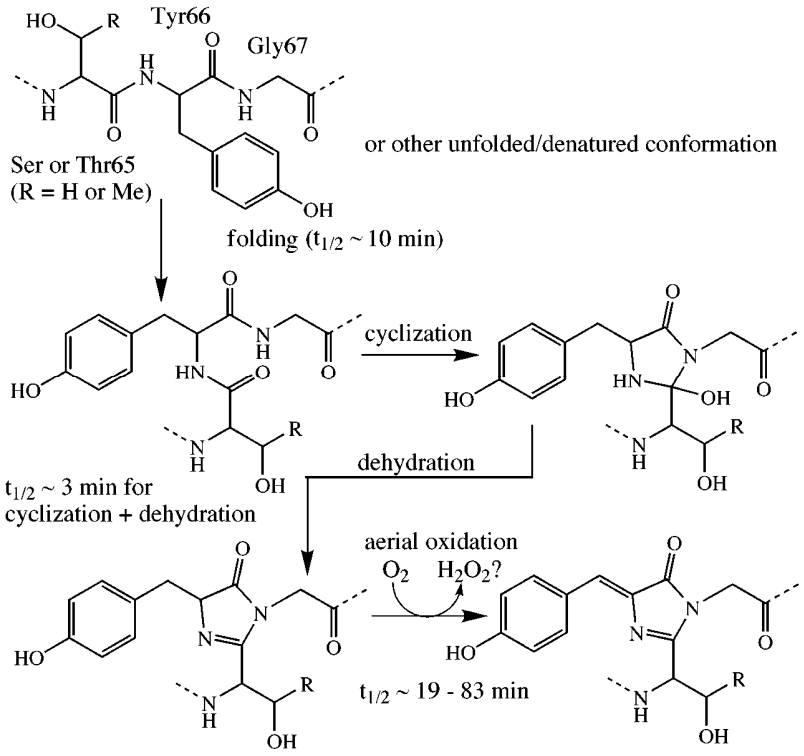

Figure 4. Chemical reaction scheme accounting for the spontaneous formation of the GFP chromophore from the Ser65-Tyr66-Gly67 motif in the native conformation of the protein in the presence of molecular oxygen (Tsien, 1998).

GFP is generally non-toxic and can be expressed to high levels in different organisms with minor effects on their physiology (Chalfie et al., 1994). Furthermore, when the gene for GFP is fused to the gene of a protein to be studied in an organism of interest, the expressed protein of interest retains its normal activity and, likewise, GFP retains its fluorescence, so that the location, movement and other activities of the studied protein can be followed by microscopic monitoring of the GFP fluorescence (Wang and Hazelrigg, 1994). Taken together, the remarkable and unexpected properties of GFP from *Aequorea victoria* summarized in this section are essential for the usefulness of GFP for studies at the molecular level of dynamic processes in living cells.

Today, there are many novel variants of GFP with improved or complementary properties in relation to those of GFP from *Aequorea victoria*, some of which will be discussed in the next section.

The GFP family and its mutants

From the perspective of its usefulness in the biosciences, some aspects of GFP function stand out. Among these are: (i) the *brightness* of the molecule, defined as the extinction coefficient at the maximum of the excitation spectrum (see Fig. 1) multiplied by the quantum yield*, i.e.* the probability that an excitation of the electronic dipole of the chromophore leads to the

emission of a photon rather than to another, heat-generating transition to the ground state of the chromophore; (ii) the photo-stability of the molecule, *i.e.* the average number of photons that the chromophore emits before the fluorescence is lost due to chemical events emanating from the first singlet excited state and leading to photo-decomposition; (iii) the existence of GFP-like molecules with different excitation and emission spectra throughout the whole visible region; (iv) rapid and efficient folding of the molecule in the intracellular context; (v) rapid maturation of the chromophore subsequent to protein folding; and (vi) monomeric configuration of GFP-like proteins, to facilitate their fusing with proteins of interest. Great brightness (i) and photo-stability (ii) are determinants of the signal-to-noise ratio of GFP-derived intracellular signals. Variable excitation and emission properties (iii) will, in particular, allow for the monitoring of events when two GFP molecules, where the emission spectrum of one (the donor) matches the excitation spectrum of the other (the acceptor), come close to each other. The principle, usually referred to as Fluorescence (or Förster) Resonance Energy Transfer (FRET), is a radiation-less energy transfer between two electronic dipoles occurring with a first-order rate constant inversely proportional to the sixth power of the distance between them. FRET can be used to estimate inter-chromophoric distances smaller than about 100Å, and the method has been generalized to involve energy transfer between three, rather than two, GFP chromophores.

Engineering of GFP from *Aequorea victoria* has led to improved brightness and photo-stability. In addition, variants with better folding properties at temperatures higher than those in the northern Pacific Ocean, the habitat of *Aequorea victoria,* have been engineered, along with GFP molecules with varying excitation and emission spectra (Tsien, 1998; Matz et al., 2002). GFP-like molecules emitting in the red part of the visible spectrum were eventually found among Antozoans (corals) (Matz et al., 1999; 2002), and made useful for intracellular protein-tagging by elimination of their oligomerizing propensity through extensive mutagenesis (Campbell et al, 2002). The coverage of the visible spectrum of light by emission spectra from GFP-like proteins existing in the year 2002 is shown in Fig. 5.

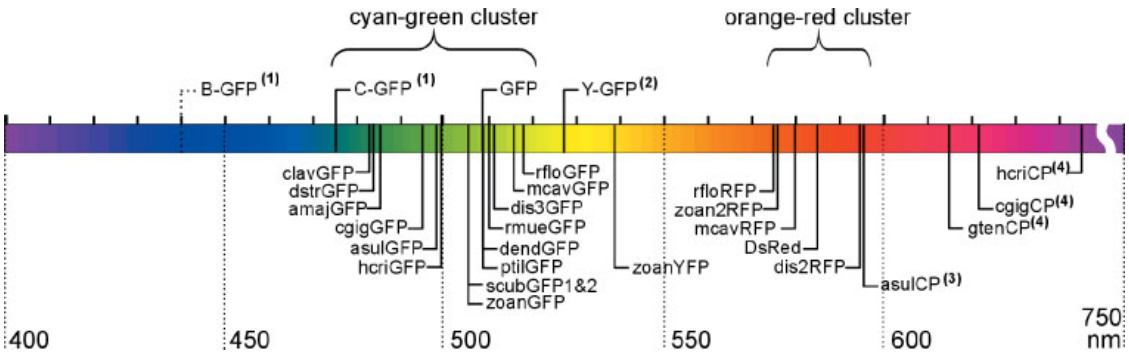

Figure 5. Spectral properties of variants of the GFP family (Matz et al., 2002).

Other important GFP-like mutants can be photo-activated from a non-fluorescent to a fluorescent state or photo-converted from one to another emission wavelength (*e.g*. Patterson and Lippincott-Schwartz, 2002; Ando et al., 2002; Tsutsui et al., 2005).

The scientific impact of GFP

Synergisms between the suitability of GFP-like proteins as precisely targeted intracellular genetic tags, the rapid development of imaging techniques, and data analysis have boosted the use of GFP in the biological sciences. Early-developed biophysical fluorescence methods like FRET (see above), fluorescence correlation spectroscopy (FCS), fluorescence cross-correlation spectroscopy (FCCS), fluorescence recovery after photo-bleaching (FRAP) and total internal reflection microscopy are now extensively used to monitor intracellular events from signals provided by the fluorescence from GFP-like proteins. In addition, fluorescence life-time imaging (FLIM), high-resolution photo-activation localization microscopy (PALM) and other high resolution methods based on GFP have emerged. Indeed, no other recent discovery has had such a large impact on how experiments are carried out and interpreted in the biological sciences, as witnessed by the appearance of more than 20,000 publications involving GFP since 1992. Some examples of GFP usage are provided below, just to indicate how GFP-based methods have radically changed the experimental potential within essentially all branches of the biological sciences.

The most common use of GFP has been to monitor the location, movement and chemical reactions involving proteins expressed as fusion partners with GFP. The localization of GFP-fusion proteins in different parts of cells, for example during the cell cycle or during exponential growth, has been extensively studied. One example is provided by the pole-to-pole oscillations of the MinDE system that determine the midpoint of bacterial cells for septum formation and cell division, as illustrated in Fig. 6.

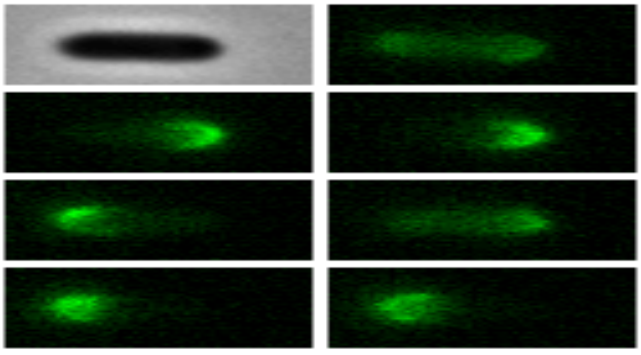

Figure 6. Pole-to-pole oscillations of GFP (green fluorescent protein) fused to MinC (following MinD) (David Fange, Uppsala, unpublished data obtained in the laboratory of J. Paulsson in Harvard, Med. School). Top row, left column: Microscope image of an *E. coli* cell. Sequence of snap-shots of the fluorescence from GFP-MinC in the *E. coli* cell at five-second intervals in the order: (left column, rows 2, 3, 4), (right column, rows 1, 2, 3, 4). The figure shows the oscillation of MinC from cell-pole to cell-

pole in a time window slightly longer than the period time of the oscillation. Through these oscillations the average concentration of the septum inhibiting MinD protein is smallest at the mid-point of the cell, which marks the mid-point for septum formation preceding cell division (Raskin and de Boer, 1999ab).

Several spectral variants of GFP tagged to different protein populations in the cell have provided data on how the dynamics of these populations respond to chemical inhibitors, mutations and gene knock outs (Ellenberg et al., 1998).

Another application is provided by monitoring the temporal expression of genes, for example in the formation of large molecular machines like the flagella and their motors, that allow for the chemotactic swimming responses of bacteria (Kalir et al., 2001).

By expressing full-length GFP-tagged proteins from their endogenous chromosomal locations at natural levels, it has become feasible to monitor the intracellular location and concentration spectrum of the whole proteasome of different organisms (Ghaemmaghami et al., 2003).

Another window for detailed kinetic studies of kinetic phenomena in cells is provided by single-cell, single-molecule microscopy based on GFP fluorescence (Xie et al., 2008). For instance, a single protein molecule bound to an immobile target in the cell can be detected as a well-defined spot, provided that its fluorescence is collected during a time shorter than the lifetime of its bound state. If, in contrast, the protein diffuses freely in the cell during the time it is monitored, then its fluorescence is hidden in the background fluorescence. This principle is illustrated by recent studies (Elf et al., 2007), of the dissociation kinetics of a GFP-fused transcription factor when bound to its specific site or to non-specific sites on the chromosome. By varying the microscope monitoring time by the use of laser pulses of different lengths, the chromosomal residence time of the factor could be determined in the two cases, and thus the rate constants for dissociation of the factor from its specific and non-specific sites.

When two proteins, one fused to a GFP with an emission spectrum overlapping the excitation spectrum of the GFP fused to the other one, interact with each other, there will be a strong FRET signal to report their union. Another way to study such direct interactions is through protein complementation with GFP. Here, one protein is fused to one half of GFP, while the other protein is fused to the other half of GFP. As the two proteins form a complex, the two halves of GFP are joined and fluorescence emerges (Cabantous et al., 2004).

An indirect way to identify protein complexes is through Fluorescence Cross Correlation Spectroscopy. Here, two proteins of interest are labelled with GFP molecules emitting light at wavelengths separate from each other. When the fluorescence intensities at these two wavelengths, resulting from laser illumination of a small volume element in a living cell, are cross-

correlated, it can be decided whether the two fused proteins diffuse independently of each other or whether they diffuse as a complex.

A number of GFP-based techniques have been used to study intracellular trafficking (*e.g.* Lippincott Schwartz et al., 2001; Phair and Misteli, 2001). Among these are the highlighting of specific protein pools after photo-bleaching or photo activation of GFP molecules. These methods have made it possible to measure the kinetics, pool sizes and residence times of proteins moving between different subcellular sites.

GFP has been used to study membrane-bound organelles, and one key finding is that many of these continuously exchange protein components with each other. For instance, the Golgi apparatus, which receives secretory cargo from the Endoplasmic Reticulum (ER), constitutively recycles its components back to the ER and disassembles during mitosis.

In the area of nuclear architectures, GFP-based studies have revealed that interphase nuclear structures are both dynamic and self-organizing.

GFP fusion proteins have been successfully used to construct sensors of intracellular parameters, like pH, Ca^{2+} or various metabolite concentrations.

Finally, GFP fusions have been extensively used for imaging cells and tissues within multicellular organisms and have become a very important experimental tool in neurobiology.

The discovery of GFP

The jellyfish *Aequorea victoria* is bioluminescent, *i.e.* it produces light with the help of chemical reactions that provide the energy for photon emission and emits green light as first described by Davenport and Nicol (1955). In 1960, Osamu Shimomura joined the laboratory of Frank Johnson at Princeton to clarify the molecular mechanism of the bioluminescence of *Aequorea victoria.* Shimomura came from Nagoya University, where he had completed extensive work on the bioluminescence of the small ostracod *Cypridina,* together with Prof. Y. Hirata. *Aequorea victoria* jellyfish were collected during the following summers in Friday Harbor in the Puget Sound of Washington state on the coast of the Pacific Ocean (Shimomura, 2005).

The active component of the *Aequorea* bioluminescence was identified as a protein, named aequorin, emitting blue light in a Ca^{2+}-dependent manner (Shimomura et al., 1962). That the light emission of purified aequorin peaked in the blue part of the visible spectrum came as a surprise, since the bioluminescence of *Aequorea victoria* is distinctly green. In the quest to explain this riddle, Shimomura and his colleagues isolated yet another protein, displaying

strong, green fluorescence (Shimomura et al., 1962). The following quotes from Shimomura et al. (1962) summarize their findings and ideas relating to GFP at this early time-point:

"A protein giving solutions that are slightly greenish in sunlight though only yellowish under tungsten lights, and exhibiting a very bright, greenish fluorescence in the ultraviolet of a Mineralite, has also been isolated from squeezates (*i.e.* extracted by squeezing out the light-emitting cells of *Aequorea victoria*). No indications of a luminescent reaction of this substance could be detected. Studies of the emission spectra of both this protein and aequorin are in progress."

and

"…it is reasonable to suppose that the greenish quality (*i.e.* of *Aequorea* bioluminescence) results from a light-filtering effect and fluorescence of the green protein which is highly concentrated together with aequorin in the photogenic cells (of *Aequorea*)."

Subsequently, Shimomura and his colleagues found that the blue luminescence from aequorin (λ_{max} = 470) (Shimomura and Johnson, 1969; Kohama et al., 1971) matches the long wavelength peak (λ_{exmax}=460 nm) in the excitation spectrum of GFP, with the emission spectrum peaking at about 510 nm (λ_{emmax} 508-515 nm) (Cormier et al., 1973). From these data, it had been suggested without direct experimental proof that the green light of *Aequorea victoria* originates in direct, radiation-less transfer of the energy of the chemically excited electronic dipole in aequorin to excite the electronic dipole of GFP, followed by green photon emission as the latter returns to the ground state (Morin and Hastings, 1971ab). In modern language, this would mean that GFP is the acceptor and aequorin the donor in an energy-transfer reaction of FRET type (see above on FRET). Experimental evidence for this hypothesis was provided by Shimomura and colleagues in a publication (1974), including estimates of the distance between aequorin and GFP in the photogenic cells of *Aequorea victoria*, along with purification protocols and detailed characterization of the absorption and emission spectra of GFP (Morise et al., 1974).

Although Shimomura's main interest was the bioluminescence of aequorin, including its use as a calcium indicator in living cells, he turned his attention to the fluorescent chromophore of GFP to clarify its chemical structure (Shimomura, 1979). He digested GFP with papain, which led to the disappearance of the fluorescence of the protein, but found one peptide fragment with the same absorption spectrum as that of the intact protein. He studied the physical-chemical properties of this peptide compared with those of a model compound, and suggested that the chromophore is a p-hydroxybenzylideneimidazolinone moiety (See Fig. 1). With access to the primary structure of GFP (Prasher et al., 1992; see below), Cody et al. (1993) re-characterized the GFP chromophore, also using Nuclear Magnetic Resonance

(NMR). They confirmed the functional portion of the chromophore as p-hydroxybenzylideneimidazolinone, as suggested by Shimomura, but re-identified the two amino acids making up the imidazolone ring as Ser and Gly (Fig. 1).

In summary, Shimomora made essential contributions to the discovery of GFP, its purification and the characterization of its physicochemical properties, including the excitation and emission spectra of its fluorescence under various conditions. He demonstrated with his colleagues that GFP can act as the acceptor in FRET from aequorin as donor, which explains why *Aequorea victoria* emits green, rather than blue, light. Finally, he correctly assigned the functional portion of the chromophore integrated in the peptide chain of GFP. Without the pioneering research of Shimomura, mainly with classical methods for protein purification and spectroscopy, it is likely that the GFP revolution would have been delayed by decades or even remained one of the hidden secrets of the Pacific Ocean.

The expression of GFP in organisms other than *Aequorea victoria*

Douglas Prasher, working in M.J. Cormier's laboratory, cloned the gene for the bioluminescent protein aequorin (Prasher et al., 1985). Using the same cDNA library from *Aequorea victoria*, Prasher and his colleagues made a first attempt to fish out the gene for GFP with DNA oligos derived from known peptide sequence elements of GFP (Prasher et al., 1992). In this way, they identified an open reading frame (ORF) encoding 168 amino acids, suggesting a molecular weight of the protein significantly smaller than that estimated earlier with other methods. This discrepancy suggested that their ORF was incomplete, but it could all the same be used to identify the three amino acids that make up the core of the chromophore of GFP (Fig. 1; Cody et al., 1993). With the help of a second cDNA library from *Aequorea victoria*, they obtained and cloned the complete ORF of GFP, encoding 238 amino acids, with the chromophore precursor motif Ser-Tyr-Gly positioned as residues 65-67 (Prasher et al., 1992). It was believed by many of the experts at the time that formation of a fluorescing chromophore in GFP would require an unknown enzyme system, idiosyncratic to *Aequorea victoria*. It was therefore considered likely that expression in heterologous systems would result in a non-fluorescent apo-form of GFP, rather than in its scientifically useful fluorescent form. At the end of their cloning article, Prasher et al. (1992) summarized their view of the prospects:

"These (cloning) results will enable us to construct an expression vector for the preparation of non-fluorescent apoGFP. Since no information is yet available regarding the biosynthesis of the chromophore, a recombinant form of this protein will be a valuable reagent with which to examine the biochemistry of chromophore formation in this unique class of proteins and the mechanism of energy transfer between aequorin and GFP".

Prasher, Ward and collaborators (Code et al., 1993; see also above) used the by then known peptide sequence of GFP (Prasher et al., 1992) to identify the tri-peptide motif responsible for

eventual formation of the functional core of its chromophore. In this, they used a similar approach with initial papain degradation of the protein to that used earlier by Shimomura (1979) and, in addition, they validated their chromophore model (Fig. 1) by NMR spectroscopy (Code et al., 1993). As mentioned above, the functional core of their chromophore was the same as that suggested by Shimomura, but they could now correctly assign Ser65 and Gly67 as the precursors of the heterocyclic imidazolidinone ring. Although the GFP chromophore was now correctly assigned, its maturation from a Ser-Tyr-Gly peptide segment in "apo-GFP" to the fluorescing GFP variant remained a mystery. They summarized the situation (Code et al., 1993):

"The posttranslational events required for chromophore formation are not yet understood. It is very unlikely that the chromophore forms spontaneously, but its formation probably requires some enzymatic machinery."

The question whether the GFP-chromophore forms spontaneously or whether its maturation requires an auxiliary enzyme system was soon to be answered, but preceding this clarification the expression of brilliantly fluorescing GFP in a selected number of model organisms was of great biological significance.

Martin Chalfie had spent post-doc time with Sidney Brenner (Nobel Laureate in Physiology or Medicine in 2002) in Cambridge, UK, working on neuron development in the small nematode (earthworm) *Caenorhabditis elegans* (*C. elegans*).

When Chalfie first heard about GFP, he was greatly excited about the prospects of using the molecular genetics worked out for *C. elegans* by S. Brenner and his colleagues to transform the organism with genes for GFP fused with a host of interesting proteins for expression under control of their authentic promoters. When affiliated at Columbia University, he obtained the GFP gene (*gfp*) clone from Prasher in 1992 after its publication (Prasher et al., 1992), and expressed it in *E. coli* the same year. The GFP protein displayed a bright, green fluorescence in this heterologous organism, suggesting that it could indeed serve as a versatile genetic marker in virtually all organisms. With the *gfp* clone obtained from Prasher, Chalfie transformed *C. elegans* with *gfp* under the control of a promoter regulating the expression of β-tubulin, abundant in six touch receptor neurons in *C. elegans*. The organism subsequently expressed GFP from distinct positions in its body and at distinct times in its development.

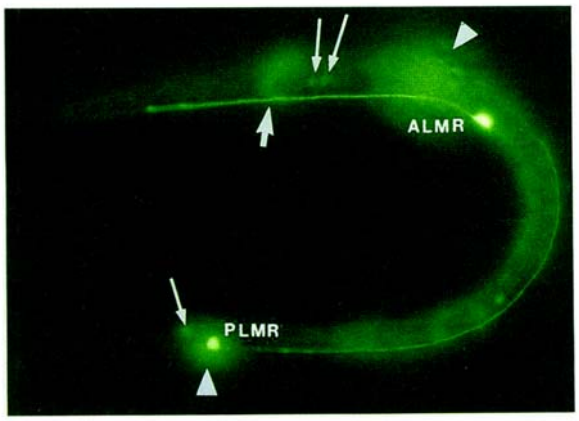

Figure 7. Expression of GFP from a first stage C. elegans larva (Chalfie et al., 1994). The two touch receptor neurons ALMR and PLMR are fluorescence-labelled at their cell bodies, leading to the strongly fluorescing two dots in the figure. Fluorescing processes can be seen projecting from both of these cell bodies. Halos produced from the out-of-focus of homologues of these cells on the other side of the animal are indicated by arrow heads. The thick arrow points to the nerve ring branch from the ALMR cell (out of focus); the thin arrows point to weakly fluorescing cell bodies.

Chalfie and his colleagues submitted their *gfp* expression results in *E. coli* and *C. elegans* to Science in mid-September 1993 and the article was published at the beginning of February 1994 (Chalfie et al., 1994). Their *C. elegans* results were also mentioned in an abstract on "A New Method of Looking at *C. elegans* Gene Expression" published in Worm Breeder's Gazette in October 1993 (Chalfie et al., 1993). The latter results were summarized as follows:

"We have developed a new way to look at gene expression in *C. elegans* (and other organisms) that utilizes an inherently fluorescent protein (the green-fluorescent protein; GFP) from the jellyfish *Aequorea victoria*. GFP fluoresces bright green when illuminated with blue light. We have found that this fluorescence does not depend upon any other component specific to *Aequorea victoria*, so gfp can be used instead of lacZ, for example, to make gene expression fusions."

The fluorescent form of GFP could be expressed not only in *E. coli* and *C. elegans* (Chalfie et al., 1993; 1994), but also in the yeast *Sacharomyces cerevisiae*, as later demonstrated by Roger Tsien and his collaborators (Chalfie et al., 1994, footnote 23) and in mammalian cells as subsequently demonstrated by Lanini and MacKeon (*Ibid*). In the same year, the possibility to use constructs of GFP fused to proteins of interest was demonstrated for yet another important model organism, namely *Drosophila melanogaster* (fruit fly) (Wang and Hazelrigg, 1994). The findings that brightly fluorescing GFP could be expressed in four very important model organisms and that GFP-fusion constructs retained both the fluorescence of GFP and the activity of the fusion partner demonstrated the virtually unlimited potential of GFP as a universal genetic tag in biological research. At the same time, the question how its chromophore maturates remained unanswered (Chalfie et al., 1994):

"…chromophore formation is not species specific and occurs either through the use of ubiquitous cellular components or by autocatalysis."

In summary, Martin Chalfie, with a *gfp* clone obtained from Douglas Prasher, was the first to demonstrate that GFP in its fluorescent form can be expressed in both *E. coli* and *C. elegans* without addition of auxiliary heterologous factors. These results meant a breakthrough in that they demonstrated the feasibility of GFP as a universal genetic marker, thereby opening the door to the universe of experimental possibilities for quantitative studies of dynamic processes in living cells that we benefit from today.

Development of GFP and GFP-like proteins

Roger Tsien expressed the *gfp*-gene anaerobically in *E. coli* and found that under oxygen-deficient conditions GFP did not fluoresce, in spite of the fact that it was expressed and apparently folded. However, fluorescence slowly emerged upon addition of oxygen to such non-fluorescent GFP molecules in living cells or in very dilute cell extracts where, in both cases, there was no *de novo* synthesis of proteins (Heim et al., 1994). From these data, Tsien and his collaborators inferred that formation of the fluorescent chromophore of GFP occurs post-translationally with molecular oxygen as the only auxiliary factor. Since molecular oxygen is ubiquitous in all aerobically living cells, their discovery explained why GFP had effortlessly fluoresced in every organism in which it had so far been expressed and strongly suggested that the same would be true for every aerobically living organism where GFP- expression was attempted. They also suggested the chemical scheme for chromophore formation (Fig. 4).

In the same paper, they introduced a number of point mutations in GFP with profound effects on its spectral properties, including variants where the main peak of the excitation spectrum of wild type GFP was shifted from the UV (Fig. 2) to the blue part of the spectrum. These engineering results showed that GFP was robust vis-à-vis amino acid substitutions, including changes in the functional portion of the chromophore (Fig. 1). They gave the start signal for all those engineering steps that have improved GFP and paved the way for its many successful applications in the biological sciences.

In these early years, Tsien and his collaborators deepened the mechanistic understanding of the fluorescence of GFP and developed several new GFP variants (Tsien, 1998) with altered spectral properties (Heim et al., 1994; Heim and Tsien, 1996), improved brightness (Heim et al., 1995) and ameliorated folding (Heim and Tsien, 1996; see also Tsien, 1998, Fig. 6).

An important step forward, allowing for rational design of mutants, was the solution of the crystal structure of GFP by Remington in collaboration with Tsien (Ormö et al., 1996) and, independently, by Yang et al. (1996).

Apart from the engineering of GFP from *Aequorea victoria*, Tsien has also made a number of important contributions to the development of variants of red fluorescent proteins, often based on the DsRed fluorescing protein from the coral *Discosoma* , discovered by Lukyanov and collaborators (Matz et al., 1999; Matz et al., 2002). Tsien and his collaborators characterized the structure of the chromophore of DsRed and the chemical steps leading to its maturation (Gross et al., 2000)**.** This work included quantum chemical computations accounting for the red-shift in the excitation and emission spectra of DsRed, compared to those of GFP from *Aequorea victoria.* He used extensive mutations of DsRed to transform it from an obligate tetramer, of limited use as a genetic tag, to a monomer with retained fluorescence properties (Baird et al., 2000; Campbell et al., 2002)**.** Recent extensions and summaries of this work by Tsien and collaborators can be found in Shaner et al., 2004; 2008. The genealogy of different proteins developed from DsRed is shown in Fig. 8:

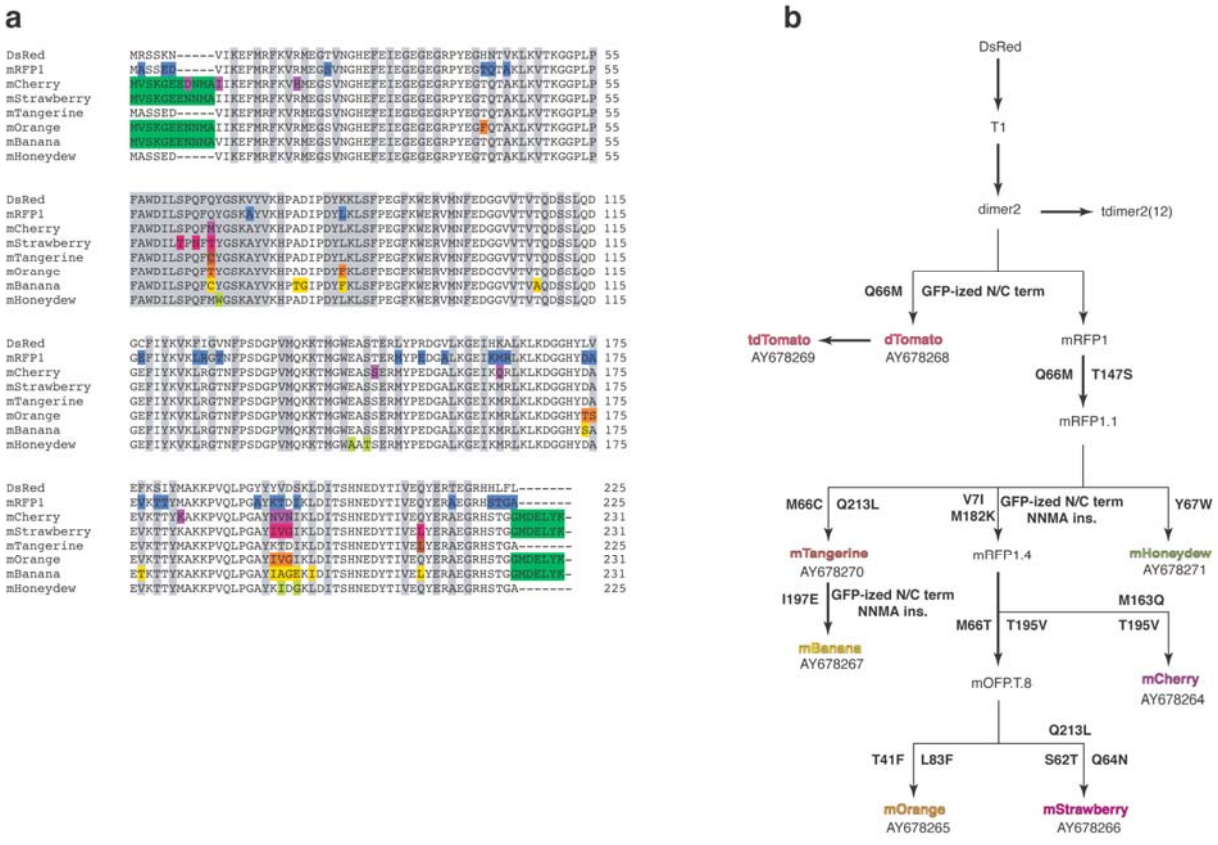

Figure 8. Genealogy of proteins derived from DsRed. 8a Sequence changes and their colours. 8b. The family tree of DsRed proteins. (From Shaner et al. 2004).

The spectroscopic qualities of these proteins are summarized in Fig. 9:

Class	Protein	Source laboratory (references)	Excitation[c] (nm)	Emission[d] (nm)	Brightness[e]	Photostability[f]	pKa	Oligomerization
Far-red	mPlum[g]	Tsien (5)	590	649	4.1	53	<4.5	Monomer
Red	mCherry[g]	Tsien (4)	587	610	16	96	<4.5	Monomer
	tdTomato[g]	Tsien (4)	554	581	95	98	4.7	Tandem dimer
	mStrawberry[g]	Tsien (4)	574	596	26	15	<4.5	Monomer
	J-Red[h]	Evrogen	584	610	8.8*	13	5.0	Dimer
	DsRed-monomer[h]	Clontech	556	586	3.5	16	4.5	Monomer
Orange	mOrange[g]	Tsien (4)	548	562	49	9.0	6.5	Monomer
	mKO	MBL Intl. (10)	548	559	31*	122	5.0	Monomer
Yellow-green	mCitrine[i]	Tsien (16,23)	516	529	59	49	5.7	Monomer
	Venus	Miyawaki (1)	515	528	53*	15	6.0	Weak dimer[j]
	YPet[g]	Daugherty (2)	517	530	80*	49	5.6	Weak dimer[j]
	EYFP	Invitrogen (18)	514	527	51	60	6.9	Weak dimer[j]
Green	Emerald[g]	Invitrogen (18)	487	509	39	0.69[k]	6.0	Weak dimer[j]
	EGFP	Clontech[l]	488	507	34	174	6.0	Weak dimer[j]
Cyan	CyPet	Daugherty (2)	435	477	18*	59	5.0	Weak dimer[j]
	mCFPm[m]	Tsien (23)	433	475	13	64	4.7	Monomer
	Cerulean[g]	Piston (3)	433	475	27*	36	4.7	Weak dimer[j]
UV-excitable green	T-Sapphire[g]	Griesbeck (6)	399	511	26*	25	4.9	Weak dimer[j]

[a]An expanded version of this table, including a list of other commercially available FPs, is available as **Supplementary Table 1**. [b]The mutations of all common AFPs relative to the wild-type protein are available in **Supplementary Table 3**. [c]Major excitation peak. [d]Major emission peak. [e]Product of extinction coefficient and quantum yield at pH 7.4 measured or confirmed (indicated by *) in our laboratory under ideal maturation conditions, in (mM • cm)–1 (for comparison, free fluorescein at pH 7.4 has a brightness of about 69 (mM • cm)–1). [f]Time for bleaching from an initial emission rate of 1,000 photons/s down to 500 photons/s ($t_{1/2}$; for comparison, fluorescein at pH 8.4 has $t_{1/2}$ of 5.2 s); data are not indicative of photostability under focused laser illumination. [g]Brightest in spectral class. [h]Not recommended (dim with poor folding at 37 °C). [i]Citrine YFP with A206K mutation; spectroscopic properties equivalent to Citrine. [j]Can be made monomeric with A206K mutation. [k]Emerald has a pronounced fast bleaching component that leads to a very short time to 50% bleach. Its photostability after the initial few seconds, however, is comparable to that of EGFP. [l]Formerly sold by Clontech, no longer commercially available. [m]ECFP with A206K mutation; spectroscopic properties equivalent to ECFP.

Figure 9. Spectroscopic and other relevant properties derived from DsRed. (From Shaner et al., 2008).

Roger Tsien has also pioneered in the development of fluorescence-based sensors of Ca^{2+} concentrations in whole organisms, tissues, organelles and submicroscopic environments, previously out of reach for quantitative monitoring (Miyawaki et al., 1999). The monitoring principle is chimeric protein constructs, consisting of a blue or cyan mutant of GFP, calmodulin (CaM) and a glycylglycine linker, the CaM-binding domain of myosin light chain kinase (M13) and a green or yellow version of GFP. When calcium ions bind to CaM, this induces the binding of CaM to M13, which reduces the distance between the two GFP variants and thereby increases the FRET efficiency. In this way, the FRET signal can be calibrated to the intracellular concentration of Ca^{2+}.

In summary, Roger Tsien has made seminal contributions to our understanding of the chemistry of the fluorescence properties of GFP and other members of the GFP family. He has made extensive contributions to the development of GFP variants with fluorescence emission in the whole visible spectrum, with increased brightness and photostability and improved folding properties along with rapid maturation of their chromophores. Roger Tsien's research has been instrumental for the development of GFP and GFP-like proteins to the highly efficient genetic tags that today constitute a universal "tool box" for studies of dynamic processes in all living systems.

References

Ando R. et al. (2002) *Proc. Natl. Acad. Sci. USA* **99** 12651-12656.

Baird, G.S. et al. (2000) *Proc. Natl. Acad. Sci.* **97** 11984-11989.

Brejc, K. et al. (1997) *Proc. Natl. Acad. Sci. USA* **94** 2306-2311.

Cabantous, S. et al. (2004) *Nature Biotechniques* **23** 102-107.

Campbell, R.E. (2002) *Proc. Natl. Acad. Sci. USA* **99** 7877-7882.

Chalfie, M. (1993) *Worm Breeder's Gazette* **13** (1) (October 1).

Chalfie, M. et al. (1994) *Science* **263** 802-805.

Cody, W.C., Prasher, D.C. et al. (1993) *Biochemistry* **32** 1212-1218.

Cormier, M.J. et al. (1973) *J. Cell Physiol.* **81** 291-297.

Cubitt, A.B. et al. (1995) *Trends Biochem. Sci.* **20** 448-455.

Davenport, D. and Nicol, JAC (1955) *Proc. R. Soc. London*, SerB **144** 399-411.

Elf, J. et al. (2007) *Science* **316** 1191-1194.

Ellenberg, J. et al. (1998) *Biotechniques* **25** 838-842.

Fradkov, A.F. (2000) *FEBS Letters* **479** 127-130.

Ghaemmaghami et al. (2003) *Nature* **16** 737-741.

Gross, L.A. et al. (2000) *Proc. Natl. Acad. Sci. USA* **97** 11990-11995.

Heim, R. et al., (1994) *Proc. Natl. Acad. Sci. USA* **91** 12501-12504.

Heim, R. et al., (1995) *Nature* **373** 663-664.

Heim, R. and Tsien, R. (1996) *Curr. Biol.* **6** 178-182.

Kalir, S. et al. (2001) *Science* **292** 2080-2083.

Kohama, Y., Shimomura, O. et al. (1971) *Biochemistry* **10** 4149.

Lippincott-Schwartz, J. et al. (2001) *Nat. Rev. Mol. Cell Biol.* **2** 444-456.

Matz, M. et al. (2002) *BioEssays* **24** 953-959.

Matz, M. et al. (1999) *Nature Biotechnology* **17** 969-973.

Miyawaki, A. et al. (1999) *Proc. Natl. Acad. Sci. USA* **96** 2135.

Morin, J.G. and Hastings, J.W. (1971a) *J. Cell Physiol.* **77** 303-312.

Morin, J.G. and Hastings, J.W. (1971b) *J. Cell Physiol.* **77** 313-318.

Morise H., Shimomura, O. et al. (1974) *Biochemistry* **13** 2656-2662.

Ormö, M. et al. (1966) *Science* **273** 1392-1395.

Patterson, G.H. and Lippincott-Schwarts, J. (2002) *Science* **297** 1873-1877.

Phair, R.D. and Misteli, T. (2001) *Nat. Rev. Mol. Cell Biol.* **2** 898-907.

Prasher, D. et al. (1985) *Biophys. Res. Commun.* **126** 1259-1268.

Prasher, D. et al. (1992) *Gene* **111** 229-233.

Raskin, D.M. and De Boer, P.A. (1999a) *Proc. Natl. Acad. Sci. U SA* **96** 4971-4976.

Raskin, D.M. and De Boer, P.A. (1999b) *J. Bacteriol.* **181** 6419-6424.

Shaner, N.C. et al. (2004) *Nature Biotechnology* **22** 1562-1572.

Shaner, N.C. et al. (2008) *Nature Methods* **5** 545-551.

Shimomura, O. (1979) *FEBS Letters* **104** 220-222.

Shimomura, O., Johnson, F.H. and Saiga, Y. (1962) *J. Cell. Comp. Physiol.* **59** 223-240.

Shimomura, O. and Johnson, F.H. (1969) *Biochemistry* **8** 3991-3997.
Shimomura, O. (2005) *Journal of Microscopy* **217** 3-15.
Tsien, R. (1998) *Annu. Rev. Biochem.* 67 509-544.
Tsutsui, H. et al. (2005) *EMBO Reports* **6** 233-238.
Wang, S.X. and Hazelrigg, T. (1994) *Nature* **369** 400-403.
Xie, X.S. et al. **(2008)** *Annu. Rev. Biophys.* **37** 417-444.
Yang, F. et al. (1996) *Nature Biotechnology* **14** 1246-1251.

Uppsala 30 September 2008

Måns Ehrenberg